Magdalena Wessely, BSc

Photozymes

Evolution of light-driven artificial enzymes for redox biotransformations

MASTER'S THESIS

to achieve the university degree of
Diplom-Ingenieur
Master's degree programme: Biotechnology

submitted to

Graz University of Technology

Supervisor
Dr. Sandy Schmidt
Prof. Dr. Robert Kourist
Institute for Molecular Biotechnology

Graz, August 2019

AFFIDAVIT

I declare that I have authored this thesis independently, that I have not used other than the declared sources/resources, and that I have explicitly indicated all material which has been quoted either literally or by content from the sources used. The text document uploaded to TUGRAZonline is identical to the present master‘s thesis.

Date	Signature

Dedicated

to

Margarete Weinzerl

(Grete-Oma)

Acknowledgments

First of all, I want to thank Prof. Robert Kourist for the opportunity to work in his superb research group and providing me with valuable recommendations and advices.

I would also like to express how deeply thankful I am for the opportunity to work with Dr. Sandy Schmidt, who thought me many lab techniques, work independently and improvement of my writing skills. I really appreciate her enthusiasms and patience as a role model.

Of course, I also want to thank Dr. Birgit Wiltschi and her working group for helping out with valuable advices and guidance.

Furthermore, I want to thank the whole Kourist group. I would never want to miss the great time I had with them. Thanks for the helpful guidance and fun times.

Special thanks go to the “Dipl. Ings to be”: Michael Runda, Andrea Nigl, Stefanie Hanreich and Kristin Bauer, for taking care of my mental health and always having my back. As well I want to thank the “inner circle”, especially Lena Skrutl, for always having fun and including me in so needed coffee breaks.

My deepest gratitude and admiration go to my parents for the love, support and giving me the possibility to explore the world in all detail and beauty. Furthermore, I really want to thank my Grete-Oma for always being there for me and being an excellent role model. I also want to thank my family and friends for always having my back and for the irreplaceable support, love and patients.

I also am deeply thankful to Julia Stadler for her support, motivation and long friendship. Thank you for always having an open ear, patience and support for me.

Finally, I want to thank Valentin Dallago for the encouragement, enthusiasm, motivation and being there for me in good and bad parts of the last (more than) 5 years.

Abstract

Over 25 % of all biocatalysts known are oxidoreductases. This class of biocatalysts is strongly used in industry due to its very broad substrate and product spectrum, and its high selectivity. A constraint of oxidoreductases, who need a nicotinamide cofactor for functional reaction, is that a regeneration of the cofactor must be performed to guarantee a sustainable and efficient biocatalytic process. This thesis aimed to establish a light-driven artificial enzyme for light-driven reduction-oxidation biotransformations. After establishing the respective constructs encoding for the model enzymes cyclohexanone monooxygenase (CHMO) and YqjM with a C-terminal His-tag, expression and purification protocols were established and optimized. The AMBER stop codon suppression technology was used for incorporation of a non-canonical amino acid into the protein scaffold to enable a strain-promoted azide-alkyne cycloaddition (SPAAC) with a photosensitizer. After generating the mutants carrying an AMBER stop codon within the respective genes, expression and purification of the obtained variants were performed. The initial specific activities of the purified wild-type model enzymes as well as for one purified CHMO variant were determined by using the well-established NADPH assay. Furthermore, light-driven biotransformation of cyclohexanone to ε-caprolactone, catalyzed by wild-type CHMO tagged with a C-terminal His-tag, was performed. In order to efficiently perform the light-driven biotransformations, a new model of a light reactor was developed. Finally, a SPAAC was performed to link the model enzyme to a photosensitizer. This study laid the foundation for the evolution of a light-driven artificial enzyme-photosensitizer complex to efficiently perform reductive-oxidative biotransformations. It is expected that an enzyme-photosensitizer complex will increase the atom efficiency and accelerates the overall reaction.

Zusammenfassung

Über 25% aller bekannten Biokatalysatoren sind Oxidoreduktasen. Diese Klasse von Enzymen wird in der Industrie intensiv genutzt, aufgrund ihres sehr großen Spektrums an Substraten und Produkten und dabei hoch selektiv sind. Eine Einschränkung bei der Verwendung von Nicotinamid Cofaktoren abhängigen Oxidoreduktasen in der Biokatalyse, ist die Regeneration dieser Cofaktoren als Voraussetzung für einen effizienten biokatalytischen Prozess. Das Ziel dieser Masterarbeit war die Etablierung eines licht-getriebenen künstlichen Enzymes für Reduktions-Oxidations-Biotransformationen. Nach der Erstellung der Plasmidkonstrukte, auf denen die Gene der Modellenzyme Cyclohexanon-Monooxygenase und YqjM codiert wurden, beide versehen mit einem C-terminalen His-tag, konnten Expressions- und Aufreinigungsprotokolle erstellt, untersucht und optimiert werden. Die Methode AMBER stop codon suppression wurde genutzt, um eine nicht kanonische Aminosäure in die Primärstruktur des Modelenzyms einzubauen, um eine strain-promoted azide-alkyne Cycloaddition des Modellenzyms mit einem Photosensitizer ermöglicht wird. Nach der Generierung der Mutanten, welche ein AMBER stop codon im jeweiligen Gen aufwiesen, wurde die Expression und Reinigung der Enzymvarianten durchgeführt. Die initiale spezifische Enzymaktivität wurde sowohl von den Wildtypen der Modellenzyme, sowie auch einer Variante der Cyclohexanon Monooxygenase mittels des gut etablierten NADPH Aktivitätstests ermittelt. Weiters wurde eine licht-getriebene Biotransformation von Cyclohexanon zu ε-Caprolacton durchgeführt, katalysiert von der Cyclohexanon Monooxygenase mit einem C-terminalen His-tag. Für diese licht-getriebene Biotransformation wurde ein neues Modell eines Lichtreaktors entwickelt. Zum Schluss wurde eine strain-promoted azide-alkyne Cycloaddition durchgeführt, um das Modellenzyme mit einem Photosensitizer zu koppeln. Diese Masterarbeit legt den Grundstein zur Entwicklung eines licht-getriebenen Enzyme-Photosensitizer-Komplexes für Reduktions-Oxidations Biotransformationen. Es ist zu erwarten, dass ein solcher Enzyme-Photosensitizer-Komplex die Atomeffizienz erhöht und die gesamte Reaktion beschleunigen kann.

Table of Contents

List of abbreviations

***dd*H2O**	double-distilled water
BVMO	Baeyer-Villiger monooxygenase
FAD	flavin adenine dinucleotide
FMN	flavin mononucleotide
NAD(P)H	nicotinamide adenine dinucleotide (phosphate)
EDTA	ethylenediaminetetraacetic acid
redox	oxidation-reduction
GOI	gene of interest
Cfe	cell-free extract
Azk	(*S*)-2-amino-6-((2-azidoethoxy) carbonylamino) hexanoic acid hydrochloride or Azidolysin
ncAA	non-canonical amino acid
w/w	weight/weight
w/v	weight/volume
v/v	volume/volume
LB	*lysogeny broth*
TB	terrific broth
TEA	triethanolamine
LED	light emitting diode
SDS-PAGE	sodium dodecyl sulfate - polyacrylamide gel electrophoresis
GC-FID	gas chromatography - flame ionization detector
conc.	concentration
MOD	modification

1 INTRODUCTION

1.1 THE INDUSTRIAL IMPORTANCE OF OXIDOREDUCTASES AS BIOCATALYSTS

The arise of new environmental priorities, such as sustainability, requires new concepts in traditional chemistry. One approach that is known as “green chemistry” is not a new technology or movement but a new perspective on chemical reactions [1]. Biocatalytic synthesis, as a major field of “green chemistry”, is gaining increased attention in industry and research. A very broad substrate spectrum, high chemo-, enantio-, regio-, and stereoselectivities combined with mild reaction conditions regarding bulk parameters such as temperature, pH and pressure, are only some of the advantages. Consequently, biocatalysis offers a new perspective and approach in contrast to traditional chemical reactions [2–5].

Biocatalysts like oxidoreductases enable access to a large number of oxyfunctionalized products which are of industrial interest by taking advantage of different incorporated cofactors, a large diversity of electron acceptors and electron-donating substrates [3]. Oxidoreductases catalyze redox reactions, whereby the exchange of electrons in or with the active site of the enzyme is the essential step to catalysis. Over 25 % of all biocatalysts used nowadays are oxidoreductases. Oxidoreductases (E.C. 1.-.-.) are classified according to their performed reaction and functional groups, as dehydrogenases, oxygenases, oxidases and peroxidases. [2].

Monooxygenases (E.C. 1.14.), belonging to the oxygenases, are of great interest for industry and find various applications. Due to their ability to incorporate one oxygen atom into a molecule, monooxygenases are used for the generation of new functional groups and selective incorporation of an oxygen atom from molecular oxygen (O_2). The second oxygen is reduced by the electrons of the nicotinamide cofactor, and water is yielded as a by-product [2]. A group of monooxygenases of high interest are Baeyer-Villiger monooxygenases (BVMOs). The mechanism of BVMOs was obtained from investigating the reaction mechanism of cyclohexanone monooxygenase from *Acinetobacter sp.* (CHMO). These enzymes are reduced by a nicotinamide cofactor in presence or absence of substrate. Molecular oxygen reacts with the enzyme-own flavin resulting in a peroxyflavin intermediate, which is stabilized by various mechanisms within the active site such as hydrogen bonds

when no substrate is available. When a substrate is present, a fast reaction with the peroxyflavin yielding the oxygenated product and water is enabled [2,6].

Another important class of oxidoreductases are ene-reductases (E.C. 1.6.). In industry, ene-reductases gained importance for the enantiopure production of pharmaceuticals and fine chemical. These enzymes contribute to different developed processes as isolated enzymes or in a multi-enzyme cascade [7]. Ene-reductases catalyze the asymmetric reduction of activated C=C bonds at the expanse of nicotinamide cofactors [8]. Ene-reductases are flavin-dependent or iron-sulfur-containing catalytically active proteins [9]. The ene-reductase YqjM, from *Bacillus subtilis*, a homologous to the old yellow enzyme, catalyzes the enantioselective redaction of keto esters [2].

1.2 LIGHT-DRIVEN BIOCATALYSIS

Enzymes that catalyze redox reactions often need the aid of several chemical compounds to transfer the electrons. These compounds are called cofactors. Many redox enzymes, such as oxidoreductases, require cofactors for their catalytical activity bound within their active site. The different cofactors transfer the needed chemical equivalents for the reaction. Cofactors, like nicotinamides, flavins or heme-groups, which are incorporated within the active site of the enzyme must be regenerated to sustain the catalytic activity of the enzyme [2,4].

It is known that traditional multi-component cofactor regeneration systems are rather complicated, consist of many reaction partners and are well established in industry. In whole-cell biocatalysis, cofactors like nicotinamides are regenerated through metabolic pathways. For instance, $NADP^+$ and NAD^+ redox carriers are involved in cellular metabolism and perform similar redox functions [10,11]. When glucose serves as carbon source, NADPH is mainly regenerated in the pentose phosphate pathway, and NADH is mainly regenerated through glycolysis and the tricarboxylic acid cycle. Nevertheless, NAD^+ is mainly used in catabolism and for respiration under aerobic conditions, while $NADP^+$ is mainly used in anabolism. These regeneration systems mainly show two disadvantages. First, the cofactors used are expensive and the regeneration is usually performed using whole-cells or enzyme attached pathways. This results in some cases in a weak atom efficiency for biocatalysis due to the significant loss of chemical energy towards other intracellular reactions, such as respiration in whole-cell biocatalysis [2,12]. Secondly, unwanted

by-products interfere with the reaction and decrease the overall yield of the desired product. Furthermore, to obtain the desired product form biocatalysis using whole-cells, it must be purified, which often includes complex and difficult protocols. Due to the numerous components involved, industry desires new and more efficient approaches. In need of a “green”, simplified, economic and advantageous approach for cofactor regeneration, the use of visible light as an energy source gained interest in organic chemistry. Using visible light enables an alternative approach to decrease the resources needed by the reduction of co-substrates and co-enzymes needed [13,14].

As described by Taglieber *et al.*, it is possible to utilize visible light as an energy donor for the regeneration of reduced flavo-enzymes. This photochemical reduction, by using inexpensive and commercially available electron donors like ethylenediaminetetraacetic acid (EDTA), opens up a more simplified system of catalysis employing oxidoreductases as shown in Figure 1 [13,15]. Taglieber *et al.* have demonstrated that photochemical regeneration of the prosthetic group of flavin-dependent oxidoreductases, like phenylacetone monooxygenase or YqjM, is in general possible. Thus, this light-driven regeneration seems to be superior, yet the reduced activity of regeneration in comparison to an enzyme-coupled regeneration system was found to be a major drawback [13].

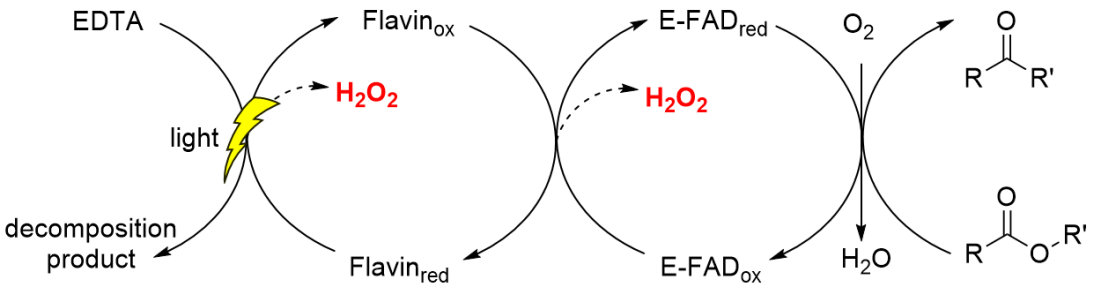

Figure 1: Light-driven cofactor regeneration using a flavin photosensitizer. The regeneration of the flavin photosensitizer by light as energy donor and EDTA as an electron donor, followed by the regeneration of the enzyme-own flavin moiety is shown. Both reactions are prone to an uncoupling reaction yielding hydrogen peroxide [13].

Inefficient electron transfer kinetics results in oxidative uncoupling from cofactor regeneration. This uncoupling from enzymatic oxidation reaction results in the formation of hydrogen peroxide due to slow electron transfer between free and enzyme-bound flavin. As a result, oxygen-dependent enzymes such as CHMO suffer from decreased activity and stability because of an elevated concentration of hydrogen peroxide in the reaction system [13,15]. For oxidative reactions using

molecular oxygen as an electron reservoir, this hydrogen peroxide is undesired for a sustainable process [14]. When oxygen-independent biocatalysts with a more accessible active site such as YqjM are used, an improvement in the light-driven reaction was found. Current studies are focused on investigation of the improvement of light-driven systems [13].

Light-driven biocatalysis is depending on the energy supplied by the visible light. As described by Hollmann *et al.*, conventional light bulbs do not provide sufficient light energy and produce heat. Conventional light-emitting diodes (LEDs) as a light source offers enough photochemical energy and can be used to ensure a more economical and efficient conversion of electrical power into visible light, while the thermal effect is strongly reduced. Due to that, less thermoregulation is needed. Furthermore, Hollman *et al.* stated that the wavelength of light was of high importance for the conversion of energy and the cofactors used. After investigation of different wavelengths, blue light (λ_{max} of 465 nm) was found to accelerate the overall reaction [16].

1.3 PHOTOSENSITIZER

Taglieber *et al.* described that flavins can be photochemically reduced and by utilizing an electron donor such as EDTA, the regeneration of the enzyme-own flavin moiety is possible. In that study, they stated that different flavins can be used, such as FAD, FMN and riboflavin. The regeneration is not strictly dependent on the type of enzyme-own flavin moiety [13]. Moreover, commercially available organic dyes have been successfully used as a photosensitizer in photobiocatalysis [17]. The advantages of fluorescence dyes are commercially available and inexpensive, they have been used initially for the strain-promoted azide-alkyne cycloaddition in this thesis [17–19].

For initial strain-promoted azide-alkyne cycloaddition, dibenzylcyclooctyne-PEG_4-5/6-FMA (*DBCO-PEG_4-5/6-FM*) was used. DBCO-PEG_4-5/6-FM is a commercially available fluorescein, which is linked by an ether linker to an octyne moiety (Figure 2). This enables not only the photosensitizer to react with the azide anion, displayed by Azk, but also provides spatial mobility to bring the photosensitizer in steric proximity to the enzyme-own flavin moiety within the active site. In respect to the model enzymes, a flavin photosensitizer will be synthesized with a linker displaying an octyne moiety to facilitate SPAAC.

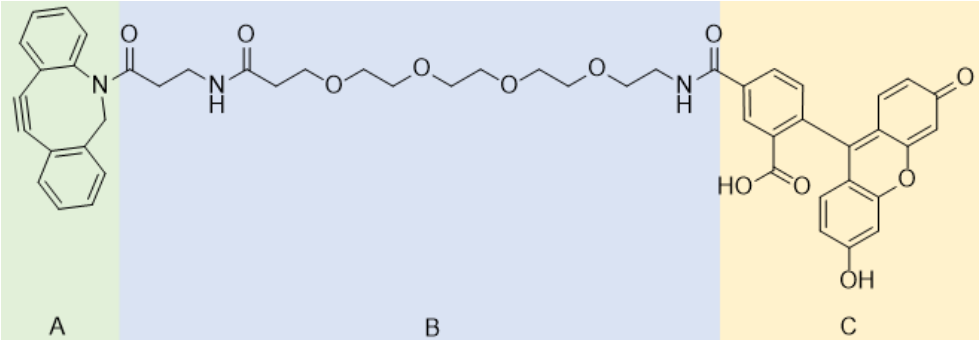

Figure 2: Dibenzylcyclooctyne-PEG$_4$-5/6-FMA consists of an octyne moiety (A) connected by an ether linker (B) to fluorescein (C) serving as a photosensitizer.

1.3.1 STRAIN PROMOTED AZIDE-ALKYNE CYCLOADDITION

Protein modification by addition of functional prosthetic groups is increasingly used in industry and research. Cycloaddition by using cysteine and maleimide, a form of protein modification, is utilized for antibody-drug conjugates. This method is based on the reaction of the functional group of the cysteine (-SH) with a maleimide, creating a thioether. Hence, the cycloaddition using cysteine and maleimide suffers from the abundance of cysteine, as well as from a long and difficult coupling process and a weak reproducibility. A site-specific modification at a distinct cysteine in a protein scaffold is not possible [20,21]. Moreover, cysteine is often involved in disulphide bonds, and the modification often leads to the loss of the enzymes secondary structure, activity and stability [22].

Another approach of site-specific coupling can be performed by Copper(I)-catalyzed azide-alkyne cycloaddition but shows major drawbacks. First, the risk of by-product formation is increased due to the high reactivity of copper, for example by interfering the reaction catalyzed by the enzyme. Secondly, the stability and activity of an enzyme can be influenced negatively. Dialysis, which is used to remove copper after the cycloaddition, decreases the activity and stability of an enzyme even more [23,24].

To preserve the enzyme properties, a copper-free click-chemistry is used increasingly. Strain-promoted azide-alkyne cycloaddition (SPAAC) is based on the exothermic cycloaddition of cyclooctyne with phenyl azide leading to a triazole. SPAAC is used for modification of molecules, for instance peptides [18]. SPAAC offers a broad biorthogonal chemical spectrum of application and was used successfully to tag glycoproteins. This copper-free form of cycloaddition is viable in prokaryotic and eukaryotic cells. Applications of SPAAC offers, in combination with

a variety of different tags, the possibility of real-time investigation and analysis of living cells [18, 24]. SPAAC was used to perform the reaction of an octyne moiety, which was covalently linked to the photosensitizer (Dibenzylcyclooctyne-PEG_4-5/6-FMA), with the azide anion (N_3^-) displayed by the ncAA Azk.

1.3.2 NON-CANONICAL AMINO ACID AZIDOLYSINE

In recent years, the application of non-canonical amino acids (ncAA) increased [26,27]. Site-specific incorporation of ncAA is used to introduce novel functionalities into the protein scaffold. The prosthetic groups of ncAAs enable a reaction with other molecules [27]. Site-specific incorporation of novel functional groups into a protein scaffold is used to alter their properties. Although many ncAAs are known, currently only a few are known by their cognate amino-acyl-tRNA synthetase and its cognate tRNA for incorporation into a functional protein scaffold [26].

The ncAA used in this experiment was (*S*)-2-amino-6-((2-azidoethoxy) carbonylamino) hexanoic acid hydrochloride or Azidolysin (Azk; CAS-Nr.: 1167421-25-1 net), as shown in Figure 3. Furthermore, the machinery for the incorporation of Azk into the protein scaffold was supplied by the vector pSCS_MmOp mentioned in this thesis [28].

Incorporation of Azk into the protein scaffold enables a copper-free SPAAC of the enzyme, containing Azk, with the photosensitizer. The octyne moiety, which is covalently linked to the photosensitizer (fluorescence dye or flavin), reacts with the azide anion (N_3^-) displayed by the ncAA Azk.

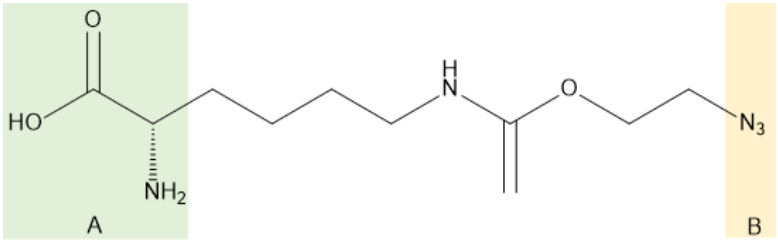

Figure 3: Azk is a non-canonical amino acid (A) displaying an azide anion (B). This ncAA was introduced into the protein scaffold to enable SPAAC with the photosensitizer.

Incorporation of the ncAA was performed site-specific into the protein scaffold. The positions for the incorporation of the ncAA were chosen for each model enzyme regarding the angle and distance to the enzyme-own flavin moiety within the active site. The positions were chosen to enable a functional electron transfer, after SPAAC, of the photosensitizer to the enzyme-own flavin moiety.

1.3.3 AMBER STOP CODON SUPPRESSION

AMBER stop codon suppression is used to introduce a ncAA site-specific into a protein scaffold. In order to facilitate the incorporation of an ncAA into a protein of choice, two important points must be addressed: Firstly, an orthogonal amino-acyl-tRNA synthetase (*o-aaRS*) and its cognate tRNA, which are encoded on the vector pSCS_MmOp, must be transferred into the host organism. Furthermore, the amino-acylated o-tRNA must be able to bind to the elongation factor TU to react with the ribosomal reaction centre. Secondly, the gene of interest (GOI) must be site-specific mutated to contain an in-frame UAG stop codon in the position where the ncAA is to be incorporated. The ncAA is loaded onto the o-tRNA by the o-aaRS. Once the ribosome reaches the mutated premature AMBER (UAG) stop codon, several cellular components, as well as the ncAA loaded tRNA, compete in interaction with the stop codon. If the o-tRNA prevails, the ncAA is incorporated into the elongating polypeptide chain, as shown in Figure 4 [28,29].

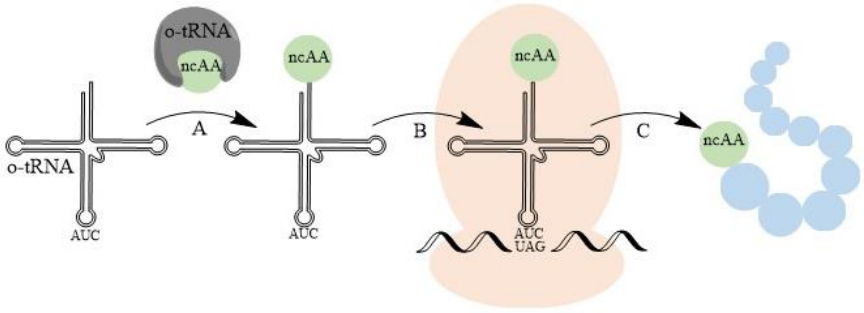

Figure 4: Simplified scheme of the translation using AMBER stop codon suppression. The o-aaRS loads the ncAA onto the o-tRNA (A), followed by the recognition of the AMBER stop codon (UAG) within the ribosome (B), resulting in the incorporated ncAA (C) in the elongating translation of the protein.

Introducing a ncAA into a protein scaffold enables to covalently bind a photosensitizer onto the folded protein by SPAAC [27,29,30].

1.4 OXIDOREDUCTASES AS MODEL ENZYMES

As mentioned above, oxidoreductases (EC 1.-) are enzymes catalyzing oxidation-reduction reactions involving an electron transfer. These reactions are of high interest for the chemical and pharmaceutical industry. Reactions performed by oxidoreductases can be the regioselective incorporation of an oxygen into a molecule but also oxidation of alcohols, aldehydes, acids and aromatic compounds as well as ketones. Most oxidoreductases require cofactors. This limits the industrial

bioprocess development because those cofactors are products of the primary metabolism of the cell. Efficient cofactor recycling is key to a sustainable economic bioprocess application of oxidoreductases [2]. Consequently, a great potential for research can be seen. Furthermore, oxidoreductases offer great model enzymes, such as cyclohexanone monooxygenase (CHMO), a Bayer-Villiger monooxygenase, or the ene-reductase YqjM, an old yellow enzyme homolog, which were used in this thesis.

1.4.1 COFACTOR REGENERATION

Oxidoreductases need different enzyme-own cofactors such as prosthetic groups like a flavin or a heme incorporated in their active site, as well as co-enzymes, such as nicotinamides. These free cofactors are serving as a hydride carrier supplying two electrons and one proton to the reaction. Free cofactors usually need regeneration through traditional multi-component systems, like whole-cell or enzyme-coupled regeneration pathways, which must be supplied with all components and resources needed. Another approach would be the addition of the cofactor directly to the reaction, yet this would have to be in stoichiometric amounts. Both forms of regeneration of the enzyme-own flavin moiety are rather expensive [2,12,14]. The disadvantage of multicomponent regeneration systems for cofactors can be overcome by chemical, electrochemical, photochemical or enzyme assisted simplified regeneration approaches. Isolated enzymes, like BVMOs, were typically investigated as model enzymes in such approaches. The use of isolated enzymes takes advantage of a better reaction control and a tolerance of higher substrate and product concentrations. Isolated enzymes must be supplied with cofactors in stoichiometric amounts for functional biocatalysis, or the cofactor must be regenerated. Chemical cofactor regeneration usually involves complex systems. The general reaction scheme includes preferred molecular hydrogen, which reduces an intermediate hybrid carrier, followed by the reduction of the cofactor. A major limitation to chemical cofactor regeneration is the low specific activity of these systems. Consequently, chemical cofactor regeneration is not sufficient compared to enzymatic approaches. Electrochemical cofactor regeneration is known as a promising alternative. This form of regeneration benefits of a mass independent electron transfer, nevertheless by-products can be formed. Limitations of electrochemical cofactor regeneration are given by the high potentials needed. Furthermore, this process is only effective in steric proximity to the electrode.

enzyme-assisted cofactor regeneration is possible by addition of a secondary substrate, converted by the same or a secondary enzyme. These secondary regeneration reactions can be catalyzed, for instance, by glucose-6-phosphate dehydrogenase or alcohol dehydrogenase. An enzyme used for the regeneration of NADPH is the phosphite dehydrogenase. The phosphite dehydrogenase catalyzes the reaction of phosphite to phosphate. Moreover, it is reported that a fusion protein of a BVMO covalently bound to the phosphite dehydrogenase results in a self-sufficient protein. All of these regeneration methods are in need of reaction partners, are constrained in their applicability and often show an inefficient atom efficiency [2].

The interest in photobiocatalysis raised because of the need for a more “green”, efficient and sustainable chemistry. Photochemistry uses visible light which is a cheap, available and an ecologically acceptable trigger for electron transfer reactions. A photosensitizer, in its light excited form, can regenerate the cofactor, as shown in a general scheme in Figure 1 above. In early studies, photosensitizer dyes, flavin dyes, organometallic compounds, metalloporphyrines or semiconductors were used as photosensitizers. Cofactor regeneration by visible light takes advantage of cheap electron donors, such as EDTA, and offers a simplified cofactor regeneration approach in contrast to the traditional multicomponent systems. Photochemical methods can offer a new more efficient approach in biocatalysis and an important topic for research [2,13,17].

1.4.2 By-product formation

Monooxygenases gained importance because of their ability to perform highly selective oxyfunctionalisation reactions. A major drawback of those reactions, involving molecular oxygen, are side reactions, where valuable reducing equivalents are wasted, and reactive oxygen species are formed. These by-products, that are usually formed due to uncoupling or unspecific catalytic activity of the enzyme, are not only increasing the demand of reduction equivalents, but also the concentration of reactive molecules within the system. The so-called uncoupling reaction occurs mainly spontaneously and different types of flavin-dependent monooxygenases suffer in different degree of uncoupling. This can be explained for flavin-dependent monooxygenases by the formation of the peroxyflavin species as an intermediate. For a functional reaction, the peroxyflavin intermediate is stabilized by several interactions within the active site. If this stabilization is insufficient, the peroxyflavin

can directly return into the initial form without substrate conversion, which releases hydrogen peroxide (Figure 5). When using a free photosensitizer to regenerate an enzyme-own flavin moiety, the risk of uncoupling is given due to the spatial positioning of the photosensitizer to the enzyme-own flavin moiety in the active site [2,31].

Reactive oxygen species can be eliminated by common enzymes in nature, such as catalase or superoxide dismutase. However, in large scale, they are not applicable, because of the amounts needed, and too expensive for industrial processes. For redox efficient processes in a large scale, the waste of reduction equivalents should be minimal. This can be achieved by protein engineering and optimizing the electron transfer. Bringing the photosensitizer in steric proximity and in an optimal angle to the enzyme-own flavin moiety will facilitate a more efficient electron transfer and overall reaction. It is expected that a high degree of simplification and increased robustness will result in a manifestly decreased probability of creation of reactive oxygen species [12,13].

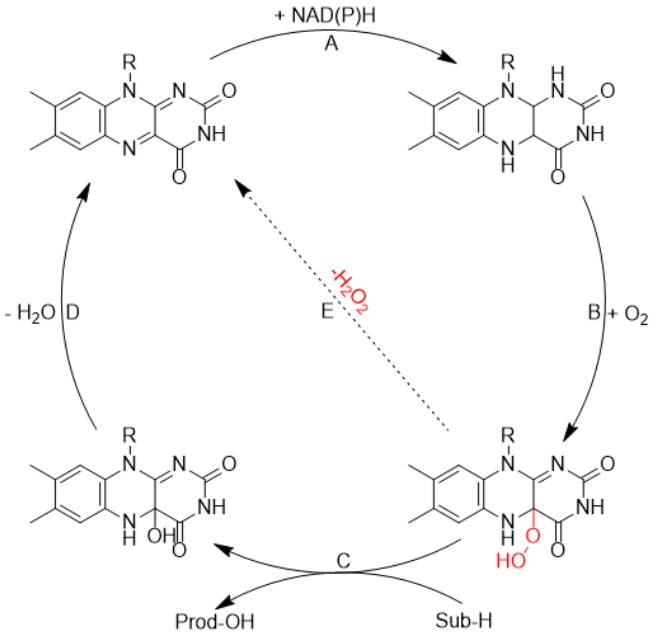

Figure 5: Reaction scheme showing the flavin moiety of a monooxygenase including the NAD(P)H depending reduction (A), the activation of the flavin with molecular oxygen to a (hydro)peroxyflavin (B), followed by substrate oxygenation (C) and yielding water as a by-product (D). In absence of substrate or weak stabilization of the (hydro)peroxyflavin the flavin moiety reacts spontaneously into its initial form, releasing hydrogen peroxide (E) [31].

This was observed for flavin-dependent monooxygenases, such as cyclohexanone monooxygenase, which was used as a model enzyme in this thesis [31]. The O_2-

dependent uncoupling of the regeneration reaction, forming undesired by-products, might be overcome or decreased significantly by cycloaddition of a photosensitizer in steric proximity to the enzyme-own flavin. Furthermore, Taglieber *et al.* described that this limitation can be overcome by small electron shuttle molecules or the use of redox-stable mediators, such as deazaflavins, to enhance the electron transfer to the enzyme-own flavin moiety might reduce the by-product formation. These limitations given the use of a second O_2-independent model enzyme for this project, such as YqjM [13].

1.4.3 CYCLOHEXANONE MONOOXYGENASE

As a model enzyme for this thesis, cyclohexanone monooxygenase from *Acinetobacter* sp. (CHMO; E.C. 1.14.13.22) was chosen. CHMO is a monomeric flavoprotein, binding a FAD in the active site. It catalyzes the conversion of the cyclic ketone cyclohexanone to the lactone ε-caprolactone by using NADPH as a cofactor and introduces oxygen into the substrate (Figure 6). This reaction is characterized by the utilization of O_2 at the expense of two-electron oxidation of NADPH and two-electron oxidation of cyclohexanone. The versatility and flexible applicability of CHMO led to an increase of research interest in it; understandably, because it not only provides a broad substrate spectrum, including cyclic ketones, thiols, aryl alkyl sulfides, cyclic thioethers or boronic acids but also the ability to introduce one oxygen asymmetrically into the substrate. This enables highly enantioselective production of lactones. Yet, Baeyer-Villiger monooxygenases such as CHMO show two major limitations when used for photobiocatalysis. One major disadvantage is the generation of reactive oxygen species, such as hydrogen peroxide. An increased concentration of reactive oxygen species reduces the stability and activity of enzymes. Furthermore, the transfer of electrons between free flavins and enzyme-bound flavins is usually slow [12,31,32]. These limitations might be overcome by positioning the secondary flavin next to the active site of the monooxygenase. This could significantly increase the efficiency of electron transfer.

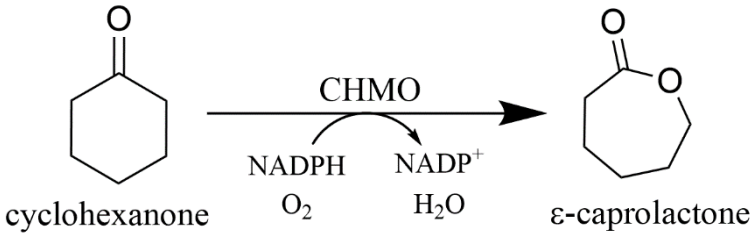

Figure 6: Conversion of cyclohexanone to ε-caprolactone catalyzed by CHMO. The monooxygenase utilizes molecular oxygen and NADPH yielding the oxygenated product and water. This model reaction was used for this thesis.

1.4.4 YQJM, AN OLD YELLOW ENZYME HOMOLOG

To overcome the limitations of CHMO due to the oxygen dependence, the old-yellow enzyme homolog YqjM from *Bacillus subtilis* (E.C. 1.6.99.1), was used as a second model enzyme for this thesis. YqjM is in aqueous solution a tetrameric ene-reductase, which binds FMN tightly noncovalent and uses NADPH as a source of reduction equivalents [32,33]. YqjM catalyzes the reduction of a double bond of α,β-unsaturated aldehydes and ketones. The oxygen-independent flavoprotein binds FMN within the active site and is more accessible from the surface [13,32,34]. Photoreduction leads to a fully reduced form of the enzyme-own flavin moiety of YqjM. Lacking formation of semiquinone indicates that the flavin environment in YqjM is different from the comparable homologous yeast and plant enzymes. Because of the broad substrate spectrum and properties of YqjM, the enzyme is of great interest for biotechnological applications in industry [32,33]. The reaction used in this experiment was the reduction of cyclohexenone to cyclohexanone (Figure 7).

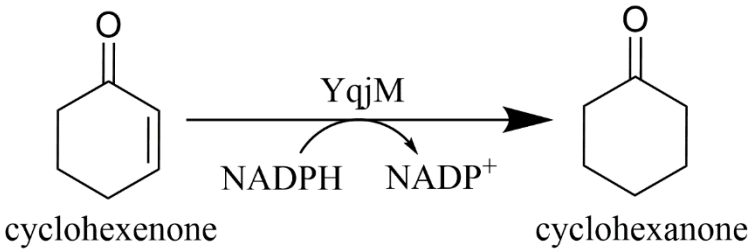

Figure 7: Conversion of cyclohexenone to cyclohexanone catalyzed by YqjM. The oxygen-independent reduction of the alkene carbon bond utilizes NADPH as a cofactor. This reaction will be used as a second model reaction in this thesis.

1.5 AIM OF THIS THESIS

The aim of the project *Photozymes* is to establish an enzyme-photosensitizer complex for light-driven biocatalysis by covalently linking a photosensitizer on the surface of an oxidoreductase (CHMO and/or YqjM), located in steric proximity to the enzyme-own flavin moiety and in a way that the catalytically active amino acid residues are not hindered (Figure 8). By bringing the photosensitizer closer to the enzyme-own flavin moiety, it is expected to overcome the limitations caused by an insufficient electron transfer between the light-excited photosensitizer and the enzyme-own flavin in the active site. This will potentially decrease or fully prevent the waste of redox equivalents in the unwanted futile cycle leading to the formation of hydrogen peroxide. Thus, we expect that in the light-driven reactions, as shown in a simplified scheme in Figure 9, the catalytic efficiency of the enzyme-photosensitizer complex will be drastically increased and higher turnover numbers will be achieved [13].

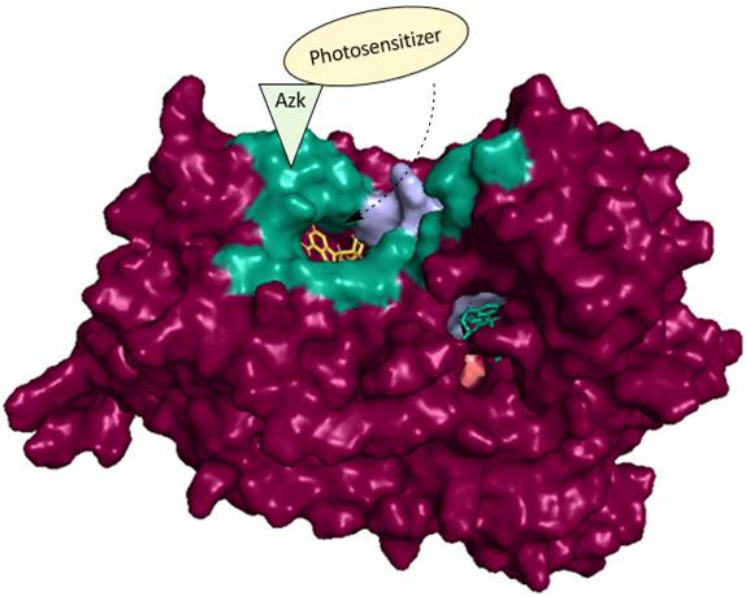

Figure 8: Simplified scheme of the enzyme-photosensitizer complex. The photosensitizer linked to a non-canonical amino acid (ncAA, Azk) via SPAAC to the azide anion. Thus, the photosensitizer is located in steric proximity to the enzyme-own flavin moiety within the active site, a more efficient electron transfer is expected. The enzyme-own flavine moiety is shown in yellow, whereas the amino acids in steric proximity to the active site are shown in turquoise. Amino acid residues used for exchange with a ncAA are shown in detail in the amino acid sequence in the Appendix (7.3 Protein sequences).

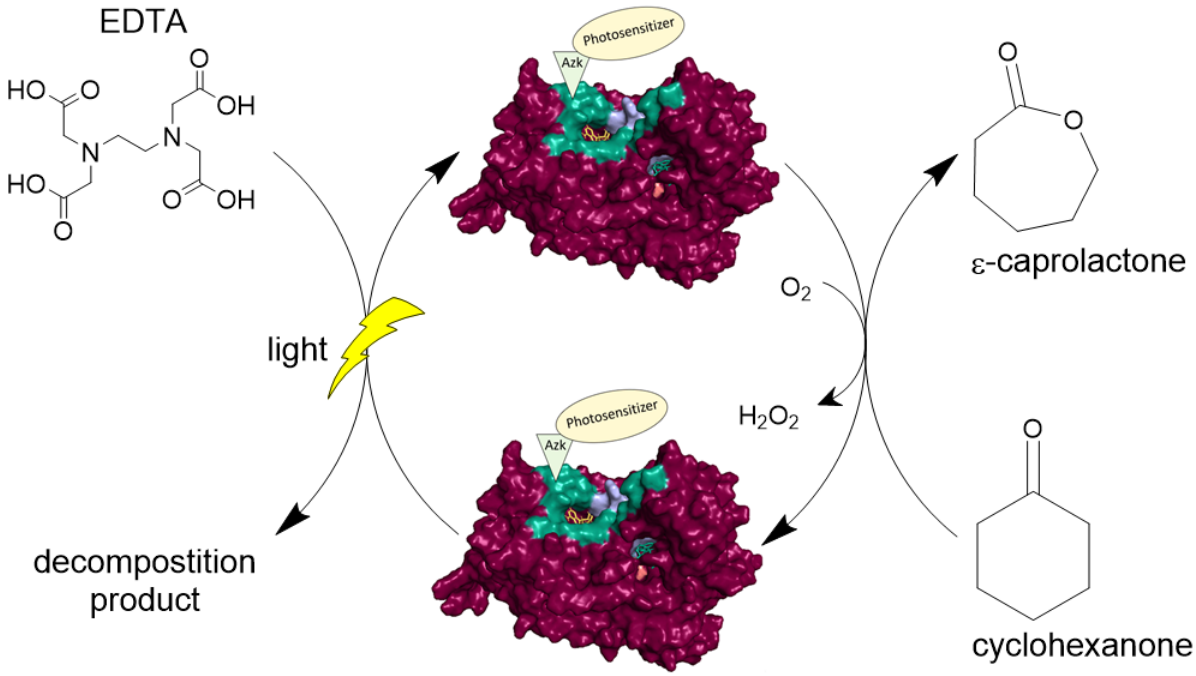

Figure 9: Aim of this project: a schematic representation of the reaction of a CHMO variant, where Azk is incorporated in steric proximity to the enzyme-own flavine moiety, linked through SPAAC to the photosensitizer, for light-driven biocatalysis. A more efficient electron transfer is expected due to the steric proximity of the photosensitizer with the enzyme-own flavin moiety.

A goal was first to generate the molecular cloned wild-type constructs for the model enzymes CHMO and YqjM encoded on the vector pSCS_MmOp. Furthermore, it was anticipated to generate the desired mutants by AMBER stop codon suppression for the genes encoding either CHMO or YqjM. Following the molecular cloning and establishment of all the constructs, it was envisaged to investigate the expression, the purification protocol and the initial specific enzyme activity. Another objective was to achieve conversion in *in vitro* photo-biotransformations using the purified wild-type CHMO. Lastly, it was aimed to link a photosensitizer to the CHMO variant, using SPAAC, with Azk incorporated into the protein scaffold at position N156 (Figure 8) [13,15,28].

2 RESULTS

1.1. MOLECULAR CLONING OF CONSTRUCTS

2.1.1 WILD-TYPE CONSTRUCTS

Successfully created constructs are shown in Table 1. All constructs were created by standard molecular cloning strategies. The general strategy for the molecular cloning was to encode a His-tag downstream of the GOI (C-terminus of the protein) to enable purification of only full transcribed proteins after using the AMBER stop codon suppression for the incorporation of the non-canonical amino acid azidolysin (Azk).

The pSCS_MmOp vector originally encodes for the green fluorescence protein under the control of a T5 promotor. This vector was used as the backbone for the constructs established in this thesis. For comparison to the original pET28a constructs that encoding the genes for CHMO and YqjM, respectively, the promotor in pSCS_MmOp was exchanged to a T7 promotor. Using a 119 bp long primer, the T7 promotor was encoded upstream of *chmo* when establishing the pSCS_MmOp_CHMO_T7 construct using Gibson assembly®. Furthermore, the construct pSCS_MmOp_CHMO_T5 was established using fast cloning, where upstream the *chmo* a T5 promotor was encoded.

A construct encoding a TEV protease cleavage site in the linker between *yqjm* and the downstream encoded His-tag was established (pSCS_MmOp_YqjMTEV_T7). It is suspected that a C-terminal His-tag attached to YqjM interferes the tetramerization due to the position of the C-terminus in the secondary structure of the folded protein. When YqjM is histidine-tagged, Fitzpatrick et al. stated that the protein has been found to exhibit a monomeric and dimeric form, instead of its native tetrameric form in aqueous solution. Consequential, the enzyme activity is most likely decreased using histidine-tagged YqjM, because the tetramerization is required for catalytical activity[32,33,35]. However, the TEV cleavage site encodes for an amino acid sequence which enables the TEV protease to cleave site-specific. This enables the cleavage of the histidine-tag. All established constructs contain a kanamycin resistance gene as a selection marker.

Table 1: List of successfully created constructs using standard molecular cloning procedures. All GOIs were tagged with a downstream encoded His-tag and all constructs contained a kanamycin resistance gene as a selection marker. All primers used for molecular cloning are listed are to be found in the Appendix under 7.1 List of primers.

construct	vector	insert	molecular cloning strategy	primers
pSCS_MmOp_CHMO_T7	pSCS_MmOp	*chmo*	Gibson assembly® [*Smi*I and *Bgl*II]	1, 2, 7 - 10
pSCS_MmOp_YqjM_T7	pSCS_MmOp	*yqjm*	fast cloning	3 - 6,
pSCS_MmOp_YqjM_TEV_T7	pSCS_MmOp	*yqjm* with TEV cleavage site	restriction/ligation [*Nde*I and *Bgl*II]	14 - 26
pSCS_MmOp_CHMO_T5	pSCS_MmOp	*chmo*	fast cloning	48-51
pET28a_CHMO_n	pET28a	*chmo*	fast cloning	40 - 43

Confirmation of each construct was done by sequencing the isolated plasmid DNA via Sanger sequencing performed by Microsynth AG (Balgach, Switzerland). All constructs showed the correct sequence, but two mismatches were found for pSCS_MmOp_CHMO_T7, indicating a point mutation leading to an amino acid exchange located downstream of the T7-promotor and a 3 bp deletion located at the downstream encoded His-tag. Constructs used for heterologous expression were used to transform *E. coli* BL21 (DE3).

2.1.2 Elimination of point mutation in pSCS_MmOp_CHMO_T7 construct

The point mutation and deletion in pSCS_MmOp_CHMO_T7, created while molecular cloning, was eliminated by using the QuikChange™ method. The point mutation of adenosine to guanine in the second position of the codon triplet at 5320 bp led to an amino acid exchange from tyrosine to cysteine. This point mutation was confirmed to be restored as shown in the sanger sequencing results in Figure 10.

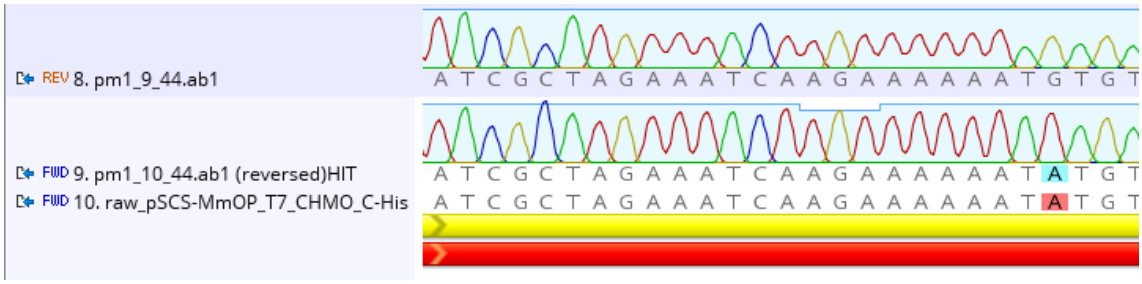

Figure 10: Confirmation of successful elimination of the point mutation in pSCS_MmOp_CHMO_T7 at construct base number 5320. The sequenced construct of Position 9 (9.pm1_10) was used for further experiments. Position 8 and 9 are showing sequencing results. Position 10 shows the original template sequence for alignment. Figure created with geneious.

After confirmation of elimination of the point mutation, the deletion of 3 bp located downstream of the *chmo* was found to result in the loss of one histidine of the encoded His-tag. This deletion was restored by the QuikChange™ method using primers which showed the correct sequence. The confirmation of the restored sequence was done by Sanger sequencing and is shown in Figure 11.

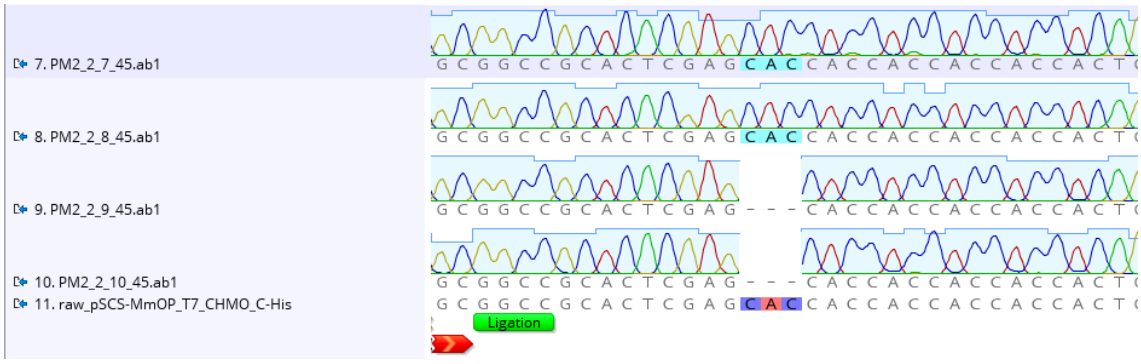

Figure 11: Confirmation of successful elimination of deletion in pSCS_MmOp_CHMO_T7 at base number 6723 – 6725. The sequenced construct of Position 7 (7.PM2_2_7) was used for further experiments. Positions 7 to10 show sequencing results. Position 11 shows the original template sequence for alignment. Figure created with geneious.

After elimination of the base exchange and the deletion, the pSCS_MmOp_CHMO_T7 construct was stored as plasmid isolate at -20 °C and used to transform *E. coli* BL21 (DE3).

2.1.3 Establishing AMBER stop codon variants

For incorporation of Azk into the model enzymes, different mutants of *chmo* and *yqjm* were generated. The positions were evaluated *in silico*, to be in steric proximity to the active site of the enzyme to enable functional electron transfer. All modified

constructs are shown in Table 2. AMBER stop codons were successfully created, using pSCS_MmOp_CHMO_T7 or pSCS_MmOp_YqjM_T7 as templates, by using the QuikChange™ method.

Table 2: List of constructs carrying an AMBER stop codon generated by the QuikChange™ method. As templates, pSCS_MmOp_CHMO_T7 and pSCS_MmOp_YqjM_T7 were used, both encoding a kanamycin resistance gene as selection marker and the respective GOI with a downstream encoded His-tag.

construct	AMBER stop codon position	insert	primers
pSCS_MmOp_CHMO_T7_AzkE127	E127	*chmo*	27, 28
pSCS_MmOp_CHMO_T7_AzkN156	N156	*chmo*	29, 30
pSCS_MmOp_CHMO_T7_AzkR389	R389	*chmo*	31, 32
pSCS_MmOp_YqjM_T7_AzkT70	T70	*yqjm*	33, 34
pSCS_MmOp_YqjM_T7_AzkK109	K109	*yqjm*	35, 36
pSCS_MmOp_YqjM_T7_AzkE335	E335	*yqjm*	37, 38

Confirmation of each construct was done by sequencing the isolated plasmid via Sanger sequencing performed by Microsynth AG (Balgach, Switzerland). The figures created with geneious can be found in the Appendix (7.4 Sequencing of AMBER stop codon variants). For each construct, 5 samples were sent for sequencing and all sequencing results were evaluated successfully.

After confirmation of incorporated AMBER stop codons, *E. coli* BL21 (DE3) was transformed with the mutant constructs. The plasmid isolations and 30 % (v/v) glycerol stocks of *E. coli* BL21(DE3) containing the different mutants of *yqjm* and *chmo* were stored at -20 °C.

2.2 HETEROLOGOUS EXPRESSION OF THE PROTEIN OF INTEREST

Heterologous protein expression was performed by using *E. coli* BL21 (DE3) cells carrying the plasmids encoding for *chmo* or *yqjm*, respectively, as GOI. The molecular weights of the model enzymes are shown in Table 3.

Table 3: Molecular weights of CHMO and YqjM, both tagged with a C-terminal His-tag.

protein	molecular weight
CHMO	62.215 kDa
YqjM	38.862 kDa

Both model enzymes were expressed for the evaluation of the specific enzyme activity. All constructs which were used for expression in this thesis are shown in Table 4.

Table 4: Constructs used for expression of heterologous protein in *E. coli* BL21 (DE3).

construct	vector	insert	his-tag
pSCS_MmOp_CHMO_T7	pSCS_MmOp	*chmo*	C-term.
pSCS_MmOp_CHMO_T5	pSCS_MmOp	*chmo*	C-term.
pSCS_MmOp_YqjM_T7	pSCS_MmOp	*yqjm*	C-term.
pSCS_MmOp_CHMO_T7_ AzkN156	pSCS_MmOp	*chmo* (Azk)	C-term.
pSCS_MmOp_CHMO_T7_AzkR389	pSCS_MmOp	*chmo* (Azk)	C-term.
pET28a_CHMO	pET28a	*chmo*	N-term.
pET28a_YqjM	pET28a	*yqjm*	N-term.

All expressions were performed in 400 mL TB medium main culture, containing 40 µg/mL of kanamycin. After cultivation, the proteins were purified using Ni-Sepharose™ beads, desalted and the initial specific enzyme activity was measured using the NADPH activity assay (to be found in section 272.3 Activity of CHMO and YqjM). Afterwards, the purified proteins were stored in 30 % (v/v) glycerol stocks at -20 °C.

Initial investigations of expression and incorporation of Azk by AMBER stop codon suppression and the SPAAC of the photosensitizer were performed only for CHMO.

2.2.1 EXPRESSION OF WILD-TYPE YQJM

Initial heterologous protein expression of YqjM was performed by using *E. coli* BL21 (DE3) cells carrying the pET28a with *yqjm* containing an upstream encoded His-tag. This construct was received from the Institute of Molecular Biotechnology Kourist-Group´s plasmid collection. Figure 12 shows YqjM with a molecular weight of 38.9 kDa after purification with Ni-Sepharose™.

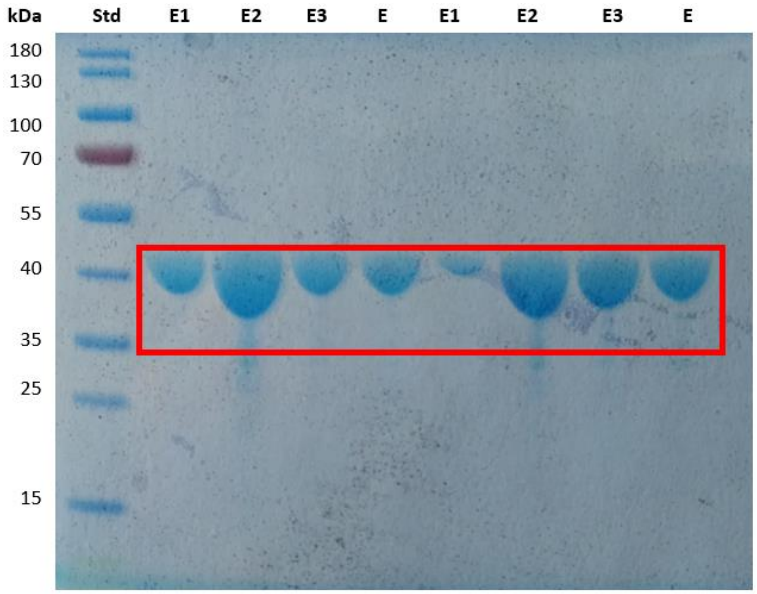

Figure 12: SDS-PAGE of the expression of YqjM investigated with *E. coli* BL21 (DE3) carrying the pET28a_YqjM. E1-E3 showing the elution of the first to third millilitre of elution buffer containing 300 mM imidazole. E shows the final desalted elution fraction that was used for the NADPH activity assay. PageRuler™ Prestained Protein Ladder, provided by Thermo Fisher Scientific (Vienna, Austria), was used as a protein standard (STD).

Within the first 3 mL of elution (E1, E2, E3) the majority of protein was detached from the Ni-Sepharose™, whereas the second elution fraction showed the most protein eluted. After desalting, the elution fraction (E) shows a significant amount of YqjM dissolved in KPi buffer (pH 6.5). This desalted elution fraction was used for determination of the specific enzyme activity by NADPH activity assay and stored afterwards in 30 % (v/v) glycerol stocks at -20 °C. The same approach was used for expression of YqjM, tagged with a C-terminal His-tag. The expression of YqjM with a C-terminal His-tag was investigated by performing an expression using *E. coli* BL21 (DE3) cells carrying the pSCS_MmOp_YqjM_T7 construct. The desalting of YqjM was performed identical to CHMO, as described in the following paragraph.

2.2.2 EXPRESSION OF WILD-TYPE CHMO

The heterologous protein expression of CHMO was performed by using *E. coli* BL21(DE3) cells. The construct pET28a encoding *chmo*, tagged with a N-terminal His-tag, was used initially for expression studies. Due to the position of the His-tag, CHMO containing the N-terminal His-tag was used for comparison not only to literature values of specific enzyme activity but also for comparison with the specific enzyme activity of CHMO when the His-tag is repositioned to the C-terminus of the protein.

During expression, two samples were taken, one at the start of induction and one 3 hours after the start of induction. For both fractions, the soluble (*s*) and insoluble (*is)* fractions were loaded onto a SDS-PAGE gel (T0-is, T0-s, T3-is, T3-s). In Figure 13, the samples taken while purification with Ni-Sepharose™ are showing various *E. coli*-own proteins. These samples were taken from the cell-free extract (Cfe), the flow-through (Rt) and from each of the four washing steps (W1-4).

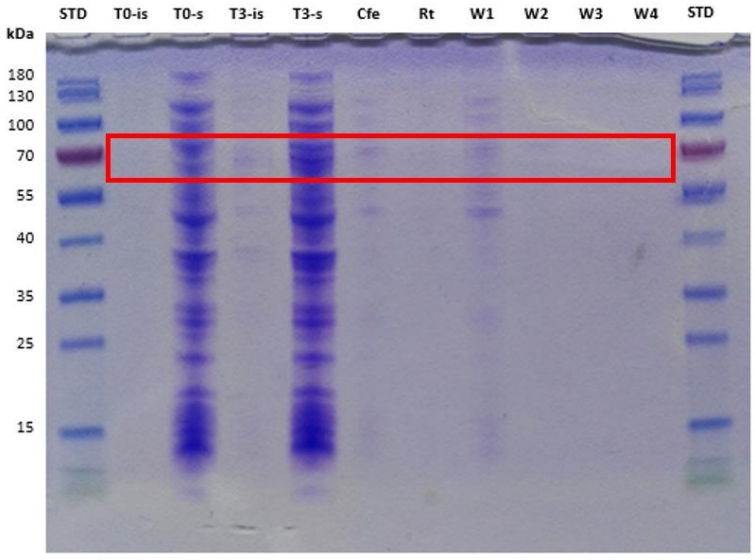

Figure 13: SDS-PAGE gel showing the expression of CHMO performed in *E. coli* BL21 (DE3) cells carrying the pET28a_CHMO. *chmo* is encoded with an upstream encoded His-tag. T0-is, T0-s, T3-is, T3-s show the soluble and insoluble fractions at the time of induction and after 3 hours of expression. Cfe shows the sterile filtrated cell-free extract, followed by the flow-through (Rt) after incubation of cell-free extract with the Ni-Sepharose™ beads. W1 to W4 show the washing fractions of the purification protocol performed. PageRuler™ Prestained Protein Ladder, provided by Thermo Fisher Scientific (Vienna, Austria), was used as a protein standard (STD).

The elution of the CHMO, containing the N-terminal His-tag was performed by incubation of 1 mL of elution buffer (300 mM imidazole) for 1 minute before

collecting the flow-through as the elution fraction 1. This step was performed seven times before performing two final elution steps with an elution buffer containing 500 mM imidazole. While the first 3 mL of elution fractions were desalted and shown in Figure 14 as E-A and E-B, the other samples were stored and directly applied onto the SDS-PAGE. With a molecular weight of 62.2 kDa for CHMO, the bands shown in Figure 14 were at the expected height.

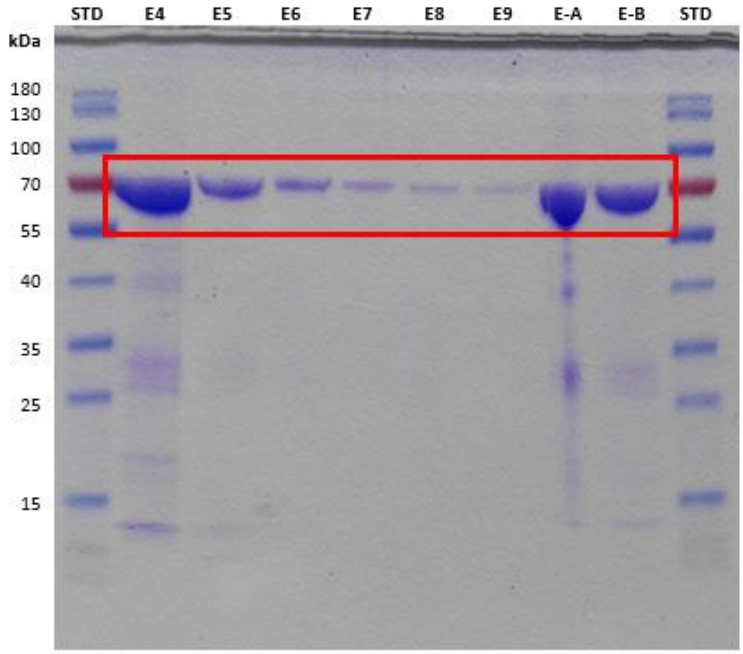

Figure 14: SDS-PAGE of the expression of CHMO investigated with *E. coli* BL21 (DE3) carrying the pET_28a_CHMO. The GOI is encoded with an upstream encoded His-tag. The first 3 mL of elution with 300 mM imidazole elution buffer were directly desalted and are shown as E-A and E-B. E4 to E7 show the elution fractions of fourth to the seventh milliliter of elution with 300 mM imidazole elution buffer. E8 and 9 show the final elution fractions using 500 mM imidazole elution buffer. PageRuler™ Prestained Protein Ladder, provided by Thermo Fisher Scientific (Vienna, Austria), was used as a protein standard (STD).

Due to the high overexpression, sufficient CHMO with a N-terminal His-tag could be obtained in the first 3 mL of elution fractions. However, CHMO could be still found after 9 mL of elution fractions were collected (as shown in Figure 14). The first three elution fractions were directly used for desalting. Samples of the desalted elution fractions (E-A, E-B) were loaded onto a SDS-PAGE gel. The remaining desalted elution fractions were combined and investigated on the specific enzyme activity by using the NADPH activity assay and were stored for further use in 30 % (v/v) glycerol stocks at -20 °C.

The pSCS_MmOp_CHMO_T7 construct established in this thesis, containing *chmo* as GOI with a downstream encoded His-tag, was used for heterologous protein expression in *E. coli* BL21 (DE3) as the host organism. The repositioning of the His-tag to the C-terminus of the protein was done in order to enable the purification of only full translated CHMO when AMBER stop codon suppression is used. It was expected that a C-terminal His-tag might lead to a specific enzyme activity decrease, but no expression limitations for the wild-type CHMO [6].

As mentioned above, samples were drawn from the expression culture at the time of induction and 3 hours after induction. These were loaded onto a SDS-PAGE gel as soluble (*s*) and insoluble (*is*) fractions, as well as the different samples, taken while purification (Figure 15).

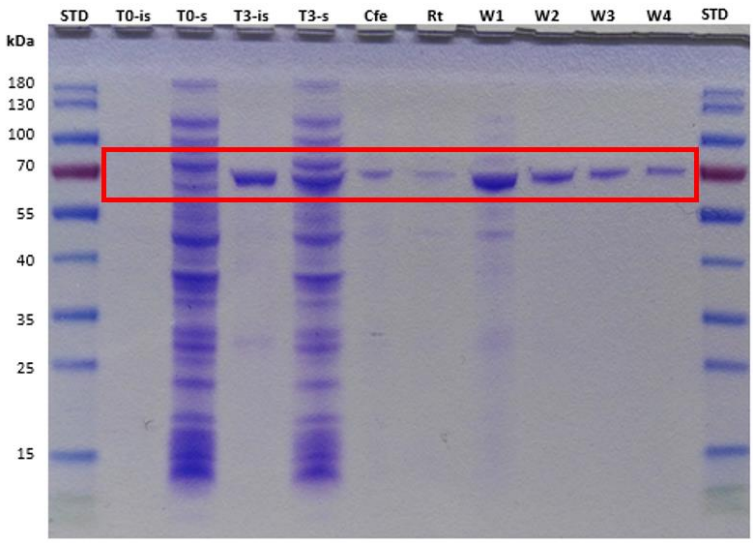

Figure 15: SDS-PAGE gel of the expression of CHMO performed in *E. coli* BL21 (DE3) cells carrying the pSCS_MmOp_CHMO_T7. T0-is, T0-s, T3-is, T3-s show the soluble and insoluble fraction at the time of induction and after 3 hours after induction. Cfe shows the sterile filtrated cell-free extract, followed by the flow-through (Rt) after incubation of cell-free extract with the Ni-Sepharose™ beads. W1 to W4 show the washing fractions samples taken while protein purification. PageRuler™ Prestained Protein Ladder, provided by Thermo Fisher Scientific (Vienna, Austria), was used as a protein standard (STD).

The elution fractions of CHMO (C-terminal tagged) were obtained as mentioned above. The SDS-PAGE gel shown in Figure 16 displays the CHMO with a size of 62.2 kDa at the expected height and successful expression of the desired protein was achieved. The first 3 mL were again desalted before loaded onto the SDS-PAGE gel (E-A, E-B).

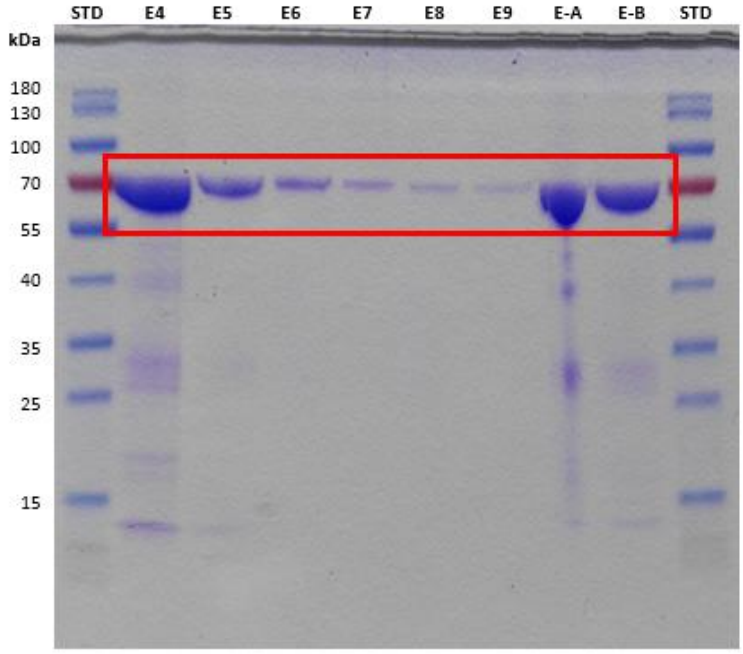

Figure 16: SDS-PAGE gel showing the expression of CHMO performed in *E. coli* BL21 (DE3) cells carrying the pSCS_MmOp_CHMO_T7. The first 3 mL of elution with 300 mM imidazole elution buffer were directly desalted and are shown as E-A and E-B. E4 to E7 show the elution fractions of fourth to the seventh milliliter of elution with 300 mM imidazole. E8 and 9 show the final elution fractions using 500 mM imidazole elution buffer. PageRuler™ Prestained Protein Ladder, provided by Thermo Fisher Scientific (Vienna, Austria), was used as protein standard (STD).

The desalted elution fractions (E-A and E-B) containing CHMO (C-terminal tag) were combined and directly used for determining the specific enzyme activity via NADPH activity assay. Afterward, the C-terminal tagged CHMO was stored in 30 % (v/v) glycerol stocks at -20 °C.

2.2.3 Expression of CHMO with AzK incorporation

After successfully establishing the three different AMBER stop codon mutants of *chmo*, encoding for the AMBER stop codon at the positions E127, N156 or R389, an initial heterologous expression study was performed. The wild-type CHMO and the CHMO_N156 variant were expressed using *E. coli* BL21 (DE3) as host organism in 400 mL TB medium containing 40 µg/mL kanamycin. The CHMO_R389 variant was expressed using *E. coli* BL21 (DE3) as expression host in 30 mL TB medium containing 40 µg/mL kanamycin and was purified using 300 µL Ni-Sepharose™ and desalted with a PD MiniTrap G-10 (GE Healthcare) column. The expression of CHMO_E127 variant was not investigated further because the 30 mL TB medium

containing 40 µg/mL kanamycin was spilled within the incubator and due to time limitations and a limited amount of Azk, repetition was not possible at this time.

The SDS-PAGE gel showed a band at the expected height of approximately 62.2 kDa, indicating a successful expression in *E. coli* BL21 (DE3) cells carrying pSCS_MmOp_CHMO_T7 construct encoding the wild-type CHMO with a C-terminal His-tag. Other unspecific bands found showing different heights indicating that those correspond to other *E. coli*-own proteins, which were able to bind onto the Ni-Sepharose™ while purification.

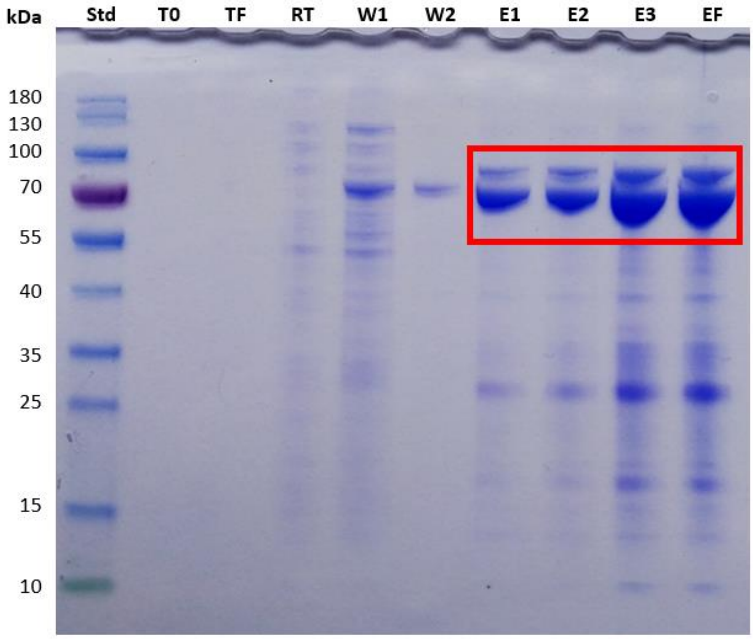

Figure 17: SDS-PAGE gel of the expression of wild-type CHMO, tagged with a C-terminal His-tag, and performed in *E. coli* BL21 (DE3) cells carrying pSCS_MmOp_CHMO_T7. This SDS-PAGE shows the samples taken at the time of induction (T0) and time of harvesting (TF), the flow-through (RT) after loading CHMO onto the Ni-Sepharose™ beads. Samples from the first two wash fractions (W1 and W2), as well as samples from the first three milliliters of elution with 300 mM imidazole elution buffer (E1-3) are shown in columns 5 to 9. The final desalted elution fraction (EF) is shown in the last column and was proceeded for further use. PageRuler™ Prestained Protein Ladder, provided by Thermo Fisher Scientific (Vienna, Austria), was used as protein standard (STD).

As expected, the expression of CHMO_N156 variant, which was performed under the same conditions as for the wild-type CHMO, was not as distinctive as the wild-type protein. Figure 18 shows the expected band at approximately 62.2 kDa indicating successful overexpression of the CHMO_N156 variant tagged with a C-terminal His-tag. In the elution fractions, other bands were found that correspond presumably to *E. coli*-own proteins which attached to the column material.

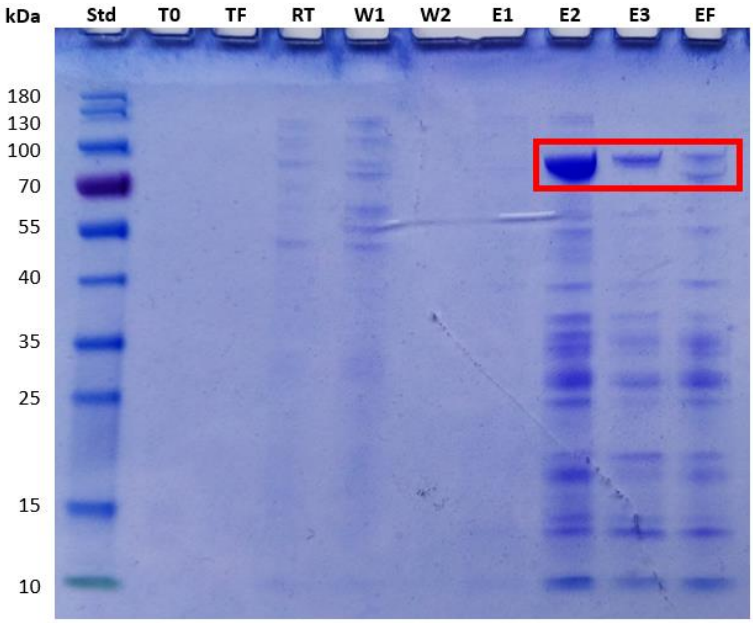

Figure 18: SDS-PAGE gel of the expression of CHMO variant, with an azidolysin incorporated at position N156, performed in *E. coli* BL21 (DE3) cells carrying pSCS_MmOp_CHMO_T7_AzkN156 construct. This SDS-PAGE shows the samples taken at the start time of the induction(T0) and time of harvesting (TF), the flow-through (RT) after loading the CHMO_N156 variant onto the Ni-Sepharose™ beads. The samples were taken from the first two wash fractions (W1 and W2) of protein purification, as well as the samples from the first three milliliters of elution with 300 mM imidazole elution buffer (E1-3) were applied onto the SDS-PAGE columns 5 to 9. The final desalted elution fraction (EF) is shown in the last column and was proceeded for further use. PageRuler™ Prestained Protein Ladder, provided by Thermo Fisher Scientific (Vienna, Austria), was used as protein standard (STD).

After purification and desalting, the wild-type CHMO and the CHMO_N156 variant were investigated by NADPH activity assay to determine the specific activities.

The expression of CHMO variant containing the AMBER stop codon at position R389 was performed in *E. coli* BL21 (DE3) used as the expression host in 30 mL TB medium main culture. The purification was scaled down to a 1.5 mL reaction tube using 300 µL Ni-Sepharose™ beads. Figure 19 shows successful expression of the CHMO_R389 variant. Due to limitations with the scaled-down purification protocol, only the band at the expected height in the elution fraction was seen. With very few *E. coli*-own proteins in the elution fraction, the successful expression of CHMO_R389 variant (62.2 kDa) could be confirmed. Nevertheless, optimization of this scaled-down purification must be done in order to have a more meaningful SDS-PAGE gel for comparison to the SDS-PAGE gel of the expression of the CHMO_N156 variant.

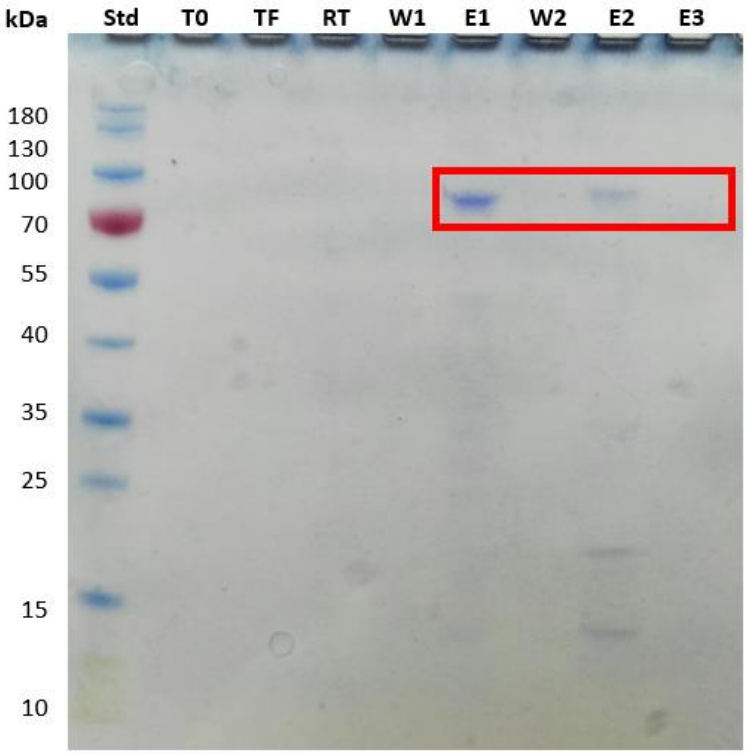

Figure 19: SDS-PAGE gel of the expression of CHMO_R389 variant, with an azidolysin incorporated at position R389, performed in *E. coli* BL21 (DE3) cells carrying pSCS_MmOp_CHMO_T7_AzkR389 construct. Expression culture of 30 mL TB medium was harvested and purified in a 1.5 mL reaction tube with 300 µL Ni-Sepharose™ beads. This SDS-PAGE shows the samples taken at the time of the induction(T0) and at the time of harvesting (TF) and the flow-through (RT) after loading the CHMO_R389 variant onto the Ni-Sepharose™ beads. Samples from the first two wash fractions (W1 and W2), as well as samples from the first three milliliters of elution with 300 mM imidazole (E1-3) were applied onto the SDS-PAGE. PageRuler™ Prestained Protein Ladder, provided by Thermo Fisher Scientific (Vienna, Austria), was used as protein standard (STD).

It can be stated that the expression of the CHMO variants N156 and R389 containing the AMBER stop codon at the respective position and having the Azk incorporated, was performed successfully.

2.3 Activity of CHMO and YqjM

The specific enzyme activities were determined by the NADPH activity assay. This was done for the different wild-type proteins carrying different His-tags (either N- or C-terminal), and for the CHMO_N156 variant (Table 5).

Table 5: Comparison of specific enzyme activity of CHMO wild-type with different His-tag positions and the CHMO variant with Azk incorporated at position N156. Activities were determined by NADPH activity assay.

enzyme	his-tag	specific activity	standard deviation	source	protein conc.
YqjM	N-term.	1-2 U/mg		Pesic et al. 2017	[1]
YqjM	N-term.	0.67 U/mg	0.0173 U/mg	this thesis	6.2 mg/mL
YqjM	C-term.	0.128 U/mg	0.007 U/mg	this thesis	2.4 mg/mL
CHMO	N-term.	4-5 U/mg		Schmidt et al. 2015	[2]
CHMO	N-term.	7.44 U/mg	0.0132 U/mg	this thesis	1.8 mg/mL
CHMO	C-term.	1.27 U/mg	0.0109 U/mg	this thesis	11.9 mg/mL
Azk N156 CHMO	C-term.	-	-	this thesis	4.7 mg/mL

The specific enzyme activity of YqjM (N-terminal His-tag) was determined with 0.67 U/mg. The repositioning of the His-tag to the C-terminus of YqjM resulted in a decrease of the specific enzyme activity of YqjM to 0.128 U/mg. This was expected due to the steric proximity of the C-terminus to the area of tetramerization of YqjM monomers [36].

The specific enzyme activity of CHMO with a N-terminal His-tag of 7.44 U/mg exceeded the literature value of 4-5 U/mg [12]. The C-terminus of CHMO is in steric proximity to the active site of the monomeric enzyme. Therefore, a decrease of the specific enzyme activity was expected when the His-tag is located at the C-terminus of CHMO. With 1.27 U/mg, the specific enzyme activity of CHMO with a C-terminal His-tag is significantly decreased. With the incorporation of Azk into the CHMO protein scaffold, a decrease of the specific enzyme activity was expected. Investigating the specific enzyme activity of CHMO_N156 variant by NADPH activity assay, no enzyme activity of the variant could be detected anymore.

2.4 LIGHT-DRIVEN BIOTRANSFORMATIONS

2.4.1 GENERAL SETUP

The light reactor built in this thesis was used in first with white light for the performed photobiotransformations. Reactions were performed in 20 mL GC vials which were put into the prepared slots of the reactor. In the following, dark reactions will refer to reactions performed under dark conditions by wrapping the reaction vials in two layers of aluminium foil. Otherwise, reactions have been performed simultaneously in the reactor to assure the same conditions. After evaluation of the first light-driven biotransformations, the light reactor was modified with conventional LED strips. These were mounted onto the middle acrylic glass panel as shown in Figure 20. The same reaction setup as for the white light approach was used with blue light.

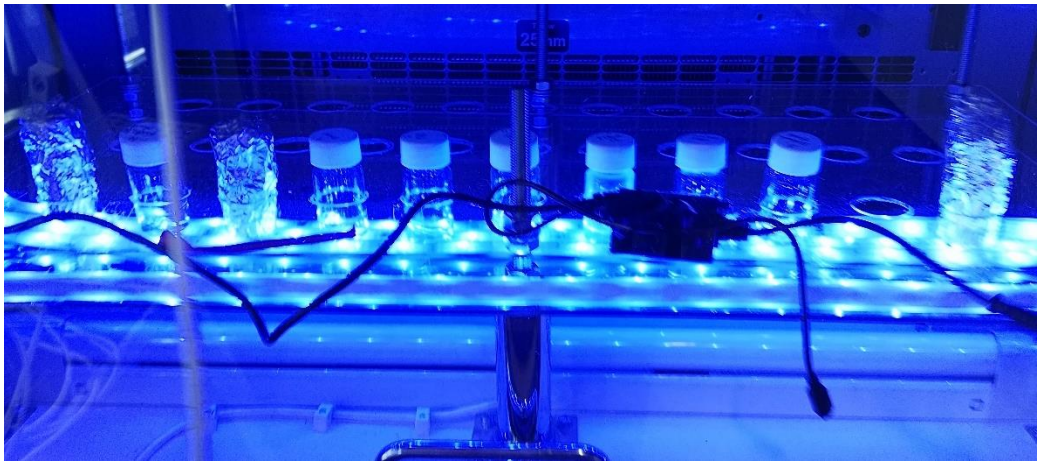

Figure 20: The light reactor setup used for light-driven biotransformations of the conversion of cyclohexanone to ε-caprolactone catalyzed by CHMO. The light reactor was modified with conventional LED strip, providing a light intensity of 34 µmol/m²s per LED, mounted on the middle acrylic glass panel. This light source enabled the adaptation of the colour of light supplied to the reaction.

The light-driven biotransformation performed in this thesis was the conversion of cyclohexanone to ε-caprolactone catalyzed by C-terminal tagged CHMO. To ensure sufficient CHMO supply, four simultaneous expressions, using *E. coli* BL21 (DE3) cells carrying the pSCS_MmOp_CHMO_T7 construct in 400 mL TB medium containing 40 µg/mL kanamycin were performed.

2.4.2 *IN VITRO* PHOTOBIOCATALYSIS USING PURIFIED CHMO

The initial approach of photobiocatalysis showed no conversion using white light. According to recent studies, blue light accelerates the overall reaction [16]. Therefore, conventional LED strips were used to modify the light reactor and enabled the use of blue light for photobiocatalysis.

Photobiocatalysis using blue light resulted in conversion when using wild-type CHMO (50 µM) with FAD (100 µM) as a cofactor and EDTA (50 mM) as an electron donor. Furthermore, an equimolar amount of catalase was added to the biotransformation reaction in order to prevent hydrogen peroxide formation.

Table 6: The detection by GC-FID of cyclohexanone and □-caprolactone is shown. The light-driven biotransformation of cyclohexanone to □-caprolactone catalyzed by CHMO WT was supplied with blue light from conventional LED strips. As a dark control reaction, a second reaction was set up using NADPH as a cofactor.

time	enzyme	cofactor	mode	cyclohexanone	ε-caprolactone
0 hours	CHMO WT	FAD	blue light	10 mM	
24 hours	CHMO WT	FAD	blue light	1.891 mM	0.235 mM
0 hours	CHMO WT	NADPH	dark	10 mM	
24 hours	CHMO WT	NADPH	dark		2.54 mM

As shown in Table 6, the light-driven reaction using FAD as a cofactor showed 0.235 mM ε-caprolactone formation after 24 hours, but still 1.891 mM of remaining cyclohexanone. Whereas for the NADPH dark control reaction after 24 hours 2.54 mM ε-caprolactone was detected but no cyclohexanone was determined.

This light-driven biotransformation and GC-FID faces two major limitations. First, the mass balance of cyclohexanone is not closed, because of the strong evaporation of cyclohexanone. Secondly, ε-caprolactone can hydrolyze to the corresponding acid and therefore, soluble in the aqueous phase. Hence the organic phase extraction

used in this experiment it is not possible to determine any loss ε-caprolactone to this hydrolyzation reaction.

Nevertheless, indicates the analysis by GC-FID a functional light-driven biotransformation of cyclohexanone to ε-caprolactone catalyzed by CHMO. As for conversion, it can be stated that the light-driven biotransformation was not as efficient as the NADPH dark control reaction. However, this is the first light-driven biotransformation that has been performed with CHMO, thus confirming that also CHMO can be driven by light.

2.5 CLICK REACTION

The incorporation of Azk into the protein scaffold by using the AMBER stop codon suppression technology was performed in order to enable the SPAAC of the photosensitizer dibenzylcyclooctyne-PEG$_4$-5/6-FMA (*DBCO-PEG$_4$-5/6-FMA*) in steric proximity to the active site of the enzyme.

The CHMO_N156 variant was used to perform an initial SPAAC with DBCO-PEG$_4$-5/6-FMA. Both components were added in equimolar concentration of 75 µM to the reaction. The cycloaddition reaction was incubated over-night. After desalting with a PD MiniTrap^{TM} G-10 (GE Healthcare, Solingen, Germany) twice, a spectroscopic detection of the enzyme-photosensitizer complex was performed.

Table 7: Fluorescence measurements of the enzyme-photosensitizer complex after SPAAC of CHMO_N156 variant with dibenzylcyclooctyne-PEG$_4$-5/6-FMA. The enzyme-photosensitizer was purified with PD MiniTrap^{TM} G-10 (GE Healthcare) twice and measured with BMG POLARstar galaxy.

sample	DBCO-PEG$_4$-5/6-FMA	fluorescence
CHMO_N156 variant	non	0.667
CHMO_N156 variant	clicked and 1 x desalted	30.334
CHMO_N156 variant	clicked and 2 x desalted	11.334

Table 7 shows that after desalting twice, the fluorescence value is still significantly higher in comparison to the CHMO_N156 variant without any DBCO-PEG$_4$-5/6-FMA. This test indicated that the photosensitizer, to be retained by size in the desalting column, was linked to the CHMO_N156 variant.

3 DISCUSSION

Oxidoreductases catalyze redox reactions and offer highly selective and robust enzymes for biocatalysis. The high chemo-, enantio-, regio-, and stereoselectivities combined with the highly divers substrate and product spectrum make oxidoreductases an important subject to research and industry[1–5]. To provide a more sustainable chemistry, light-driven biocatalysis is increasingly gaining importance [13]. This thesis aimed to establish an enzyme-photosensitizer complex to simplify the regeneration of the enzyme-own flavin moiety of flavin-dependent oxidoreductases. The project was subdivided into a) molecular cloning and expression of wild-type model enzymes (CHMO and YqjM), b) the modification of these model enzymes by using AMBER stop codon suppression technology and the expression of CHMO variants with Azk incorporated, c) set up of *in vitro* photobiocatalysis using purified wild-type CHMO and d) SPAAC of the photosensitizer with the CHMO_N156 variant, which had a Azk incorporated at position N156.

3.1 MOLECULAR CLONING AND EXPRESSION

Using pSCS_MmOp as a vector system for this experiment enabled the simplification of transforming an *E. coli* cell with only one plasmid. The vector already encoded for the machinery needed for AMBER stop codon suppression. This vector, kindly provided by Dr. Birgit Wiltschi from the acib GmbH (Graz, Austria [28]), was used for molecular cloning as a backbone. The genes encoding *chmo* and *yqjm* were received from the plasmid collection of the Institute of Molecular Biotechnology (Graz University of Technology, Austria), encoded on pET28a vectors. Since the pET28a constructs contain a T7 promotor, the T5 promotor of pSCS_MmOp upstream of the GOI was exchanged for the stronger T7 promotor. This enabled the comparison of the expression of the model enzymes tagged with the N-terminal His-tag encoded on the pET28a constructs with the model enzymes tagged with a C-terminal His-tag encoded on the pSCS_MmOp constructs generated within this thesis. After successful molecular cloning of all constructs, the sequences of the cloning sites were confirmed by sanger sequencing.

The pSCS_MmOp_CHMO_T7 construct showed two mismatches when sequenced. These may have emerged spontaneously due to malfunctions during molecular cloning. The mismatches indicated for a point mutation downstream the

promotor within the *chmo* and a deletion of 3 bp downstream of *chmo*, which indicated to the deletion of the first codon encoding for the His-tag. These errors were restored using QuikChange™ mutagenesis by using primers containing the correct sequence. Only constructs with a confirmed correct sequence were used for introduction of the in-frame AMBER stop codons by QuikChange™ mutagenesis and subsequent expression studies of the created enzyme variants.

Although both model enzymes, CHMO and YqjM, use flavin cofactors and an enzyme-own flavin moiety within the active site and therefore were chosen to serve the model enzyme, this thesis further concentrated on the investigation of CHMO as a model enzyme [6,32,33,37]. The monomeric and O_2-dependent CHMO was chosen because it serves as a model enzyme to investigate the reduction of the unwanted uncoupling reaction, at the flavin cofactor and the enzyme-own flavin moiety, when a photosensitizer is directly coupled in steric proximity to the active site [6]. Whereas YqjM is O_2-sensitive and the concentration of oxygen interferes with the reaction performed by the ene-reductase. This was overcome for determination of the initial specific enzyme activity by adding glucose and *glucose oxidase* to the performed NADPH activity assay. Furthermore, YqjM exhibits the constrain of building the active site by tetramerization in aqueous solution. This tetramerization site is found to be in steric proximity to the C-terminus. Tetramerization and specific enzyme activity can be therefore face limitations when a C-terminal His-tag is used [7,32,35,36]. Thus, CHMO chosen as main model enzyme. It is expected that the efficiency of light-driven biotransformation using a CHMO-photosensitizer complex as catalyst can be improved and in correlation the unwanted uncoupling reaction reduced. Initial light-driven biotransformation using wild-type CHMO showed low conversion, which indicated the need of investigation of improvement.

Therefore, CHMO was prioritized as model enzyme and successful expression of wild-type CHMO, but as well of the CHMO variant carrying an Azk at position N156 and of the CHMO variant carrying an Azk at position R389 performed. The SDS-PAGES showed a band at the expected hight. This indicates that the *chmo* mutants, containing the AMBER stop codon, were fully translated into the 62.2 kDa CHMO variants. For the initial investigation of specific enzyme activity investigation, the N156 CHMO variant was chosen.

Nevertheless, wild-type YqjM was expressed, purified and desalted. The SDS-Page of YqjM showed only the bands at expected hight with no indication of *E. coli*-own proteins purified with the enzyme. This initial expression of YqjM was used to establish an expression, purification and desalting protocol to be used in further studies.

The next steps in this project will include a simultaneous expression of all variants of both CHMO and YqjM, including one cultivation supplying Azk at the time point of induction, and one cultivation where no Azk will be supplied. This will give information which position of Azk incorporation into the protein scaffold yield catalytically active model enzymes. Furthermore, the catalytic activities of the variants can be compared and the most active variant of each model enzyme can be chosen for further investigation. Moreover, a simultaneous expression under the same conditions for the wild-type model enzymes must be performed. These relevant benchmarks will be done to ensure the validation and comparison of the variants with the wild-types of the model enzymes. To confirm a successful expression of the variants and incorporation of Azk, the translated protein must be analyzed by mass spectroscopy. Using AMBER stop codon suppression some limitations during the expression of the enzyme variants were expected. Due to the in-frame stop codon and competing tRNAs, an abort of translation can occur at this AMBER stop codon. This results in non-catalytic fragments of the model enzyme [26,27]. As those fragments are not desirable and result in unnecessary consumption of amino acids, the His-tag was encoded downstream of the GOI. This enabled the purification of only fully translated proteins, which provided the possibility of coherent calculation of the specific enzyme activity when determined.

The analysis of expression of the CHMO variants showed the expected bands on the SDS-PAGE gel. Nevertheless, other bands were found, indicating different sized proteins. These might correspond for *E. coli*-own proteins which were bound by the Ni-Sepharose™ beads during purification. A possible explanation would be that the charged Ni- Sepharose™ is able to bind other proteins, especially when low concentrations of the His-tagged proteins are already bound to the Ni-Sepharose™ beads. A possible solution would be to decrease the amount of Ni-Sepharose™ beads used adjusted to the level of expression. The optimization of purification may include the performance of additional washing steps and a primary elution step with less than 300 mM imidazole in the elution buffer.

3.2 SPECIFIC ENZYME ACTIVITY

The initial specific enzyme activity was determined by performing a NADPH activity assay. In this thesis, it was shown that a relocation of the His-tag led to a decrease of specific enzyme activity. CHMO with N-terminal His-tag showed a specific enzyme activity of 7.44 U/mg. The C-terminally tagged CHMO showed a specific enzyme activity of only 1.27 U/mg, resulting in a decrease of 83 %. This decrease in specific enzyme activity can be explained by the steric proximity of the C-terminus of the protein to the active site. The additional amino acids can hinder an efficient substrate positioning within the active site of the enzyme [6]. YqjM showed an activity of 0.67 U/mg, when a N-terminal His-tag is present. Repositioning the His-tag to the C-terminus of YqjM led to a decrease of the specific enzyme activity of 81 % to 0.128 U/mg. This can be explained by the position of the C-terminus in the secondary structure of the His-tag to the tetramerization region of the YqjM tetramer when dissolved in aqueous solution, as well as the steric proximity of the C-terminus to the active site of YqjM [32,33,36]. To enhance the specific enzyme activity, the protein must always be purified sufficiently and all steps of harvesting, purification and desalting of the protein must be performed at around 4 °C or on ice.

It was expected that the incorporation of the ncAA Azk leads to a further decrease of the specific enzyme activity of CHMO. After incorporation of Azk into CHMO variant N156, a NADPH activity assay was performed, but no specific enzyme activity was determined, although the protein was handled at the same conditions as the wild-type proteins. This might indicate that the incorporated Azk interferes with the catalytical activity. This can be due to the properties of Azk, which shows a molecular weight of 259.3 g/mol compared to the original asparagine, with 132.1 g/mol, at this position. The incorporation of the ncAA into primary structure of the protein could interfere the establishment of the correct secondary structure, because of the azide anion displayed by Azk. Furthermore, Azk displaying an azide anion is displaying a higher reactivity and could interfere the catalytical activity at the active site of the enzyme. To investigate the impact of the incorporation Azk, further expressions of the different variants of both model enzymes must be performed. The NADPH activity assays performed with the different model enzyme variants will indicate for the best position for incorporation of Azk and minimize the decrease of the specific enzyme activity.

In order to enable functional light-driven biotransformation, major limitations are the enzyme activity and stability. To perform light-driven biocatalysis catalyzed by an enzyme-photosensitizer complex, the stability of the complex must be increased to obtain an active catalyst throughout the duration of the performed reaction [2]. Furthermore, it is expected that with a catalytical active enzyme-photosensitizer, higher specific enzyme activity can be achieved due to a more efficient electron transfer. This will hopefully increase the atom efficiency of the overall reaction [13].

3.3 PHOTOBIOCATALYSIS

For the initial light-driven biocatalysis that has been performed using wild-type CHMO and white light, no conversion was detected after 24 hours. Nevertheless, the dark control performed for this experiment, using NADPH as a cofactor, showed conversion of cyclohexanone to ε-caprolactone catalyzed by CHMO.

By replacing the fluorescent lamp that initially served as a light source with conventional LED strips which supplied blue light to the reaction, it was possible to detect conversion in the light-driven biotransformation within 24 hours. This light-driven biotransformation was the first one performed with CHMO as a catalyst. Yet, it can be stated that in this thesis no full conversion in the light-driven biotransformation was achieved using the reaction system described by Taglieber *et al..* Taglieber *et al.* performed successful light-driven biotransformation using a mutant phenylacetone monooxygenase from *Thermobifida fusca*, which is a flavin-dependent BVMO [6,13]. The limited conversion achieved using wild-type CHMO however is a proof of concept; yet it must be enhanced significantly and limitations must be overcome to accomplish a full functional light-driven biotransformation. Limitations of light-driven biotransformation can be subdivided.

Firstly, the specific enzyme activity is decreasing over time due to the enzyme stability and is negatively influenced by a possible build-up of reactive oxygen species. The possibility of hydrogen peroxide production, through uncoupling reaction, was prevented by the addition of catalase to the reaction.

Secondly, the energy supplied by the light source gives limitations to the reaction system. As stated above, the conversion of cyclohexanone to ε-caprolactone was achieved using blue light in the light-driven biotransformations using FMN as a

cofactor, whereas no conversion by the light-driven biotransformations using other photosensitizers, such as fluorescein and FAD, was detected.

Nevertheless, FMN was already successfully used as reaction partner in light-driven biotransformations, as described by Taglieber *et al*., and it has been reported that fluorescent dyes can offer cheap and commercially available photosensitizer, although no conversion was detected in this work using fluorescein as a photosensitizer [13,17]. This leads to the assumption that the energy supplied by the light must be adjusted to the photosensitizer used. Furthermore, although small closed reaction systems were used, the evaporation of cyclohexanone could not be fully prevented. Moreover, ε-caprolactone can hydrolyze to its corresponding acid and cannot be extracted by organic phase extraction without acidification, which was not done for this experiment. This resulted in a not fully closed mass balance of the reaction, and thus only low concentrations of cyclohexanone and ε-caprolactone were detected by GC-FID. The results of this thesis support the findings of Taglieber *et al.*, but also showed that light-driven biotransformations must be optimized to reach efficient conversion [13,16,17]. To achieve full conversion, a promising approach would be an increased concentration of CHMO supplied to the reaction or decreasing the amount of cyclohexanone added to the reaction. To facilitate a fully functional light-driven regeneration of the enzyme-own flavin moiety, the balance between the concentration reaction components, reaction systems and light supply must be further investigated in the future.

Nevertheless, the aim of this thesis was to facilitate a more efficient regeneration of the enzyme-own flavin moiety. The successful performed light-driven biotransformations using FMN as a photosensitizer indicates that FMN is a promising photosensitizer for the planned cycloaddition of a photosensitizer in steric proximity to the active site of the enzyme. It is intended to synthesize a FMN connected via a linker to an octyne moiety. This enables a site-specific SPAAC of FMN to the enzyme variant displaying an azide anion of the incorporated ncAA.

3.4 LIGHT REACTOR

The light reactor constructed in this thesis was designed to offer multiple slots for different sizes of reaction vials. For each size of vials used, a separate top acrylic glass panel with fitting bores was prepared. Due to the spacing of the acrylic glass panels, air circulation is given, which prevents heat build-up. One major

disadvantage of this light reactor is the distribution of the three light sources. The intensity of light varies throughout the different positions of the reaction vials. This might lead to enhanced bleaching in the center from where the intensity of the light decreases to the sides of the reactor due to a higher exposure during the reactions. In this thesis, this was overcome by addition of conventional LED strips onto the middle acrylic glass panel positioning one LED below the bottom of each reaction vial. No heat build-up was observed due to the ventilation by the incubator. By using the conventional LED strips as the only light source, it was also possible to adjust the colour of light to facilitate a functional light-driven biotransformation [12,16,38]. Besides the advantage of colour adjustment and even distribution of light sources, the LEDs are far more energy efficient and thus of economic and ecologic considerable advantage [16]. This light reactor enables the performance of different light-dependent reactions using whole-cells or purified enzymes.

3.5 STRAIN-PROMOTED AZIDE-ALKYNE CYCLOADDITION

In this study, a strain-promoted azide-alkyne cycloaddition was performed to link the photosensitizer to the CHMO_N156 variant displaying an azide anion by a ncAA at position N156 in steric proximity to the active site. To separate the enzyme-photosensitizer complex from free photosensitizer a buffer exchange was performed. The fluorescence values indicated the reduction of photosensitizer concentration throughout the buffer exchanges. The measurements of fluorescence indicated that the SPAAC was successful. However, a mass spectroscopic analysis of the enzyme photosensitizer complex is yet to be done to verify a successful cycloaddition.

This initial study indicated successful incorporation of Azk and that a SPAAC is most likely possible. This supports the findings of previous studies, where SPAAC was already successfully used for molecular labelling [18,19]. Nevertheless, a successful cycloaddition of the enzyme with a photosensitizer must be verified by mass spectroscopy.

4 CONCLUSION AND FUTURE PERSPECTIVES

This study laid the foundation for the further evolution of a light-driven artificial enzyme for redox biotransformations. The monooxygenase CHMO and the ene-reductase YqjM were chosen as model enzymes to create an enzyme-photosensitizer complex for light-driven biocatalysis. The establishment of constructs needed was successful, and it was possible to express and purify the wild-type model enzymes. The respective genes encoding for CHMO and YqjM, respectively, were under the control of a T7 promotor and encoded with a downstream encoded His-tag, resulting in a C-terminal His-tag at the translated protein of interest. After introducing in-frame an AMBER stop codon in the GOIs encoding for the respective model enzymes, the variants were expressed with incorporated Azk into the protein scaffold by AMBER stop codon suppression.

Initial specific enzyme activity was determined by NADPH activity assay. It was shown that specific enzyme activity is decreased if the His-tag is repositioned to the C-terminus of the translated model enzymes. However, no specific enzyme activity was determined for the CHMO_N156 variant having Azk incorporated into the protein scaffold at position N156.

A light-driven biotransformation with wild-type CHMO carrying a C-terminal His-tag as biocatalyst and FMN as a photosensitizer was performed and the conversion of cyclohexanone to ε-caprolactone was determined by GC-FID analysis. Furthermore, an initial strain-promoted azide-alkyne cycloaddition was performed with the CHMO_N156 variant and DBCO-PEG$_4$-5/6-FMA. Although the variant and the enzyme-photosensitizer complex still need to be verified by mass spectroscopy, the fluorescence values determined in this study indicated a successful strain-promoted azide-alkyne cycloaddition.

The next steps within the project *Photozyme* will be an assessment of all mutant constructs generated in this thesis. The aim would be to establish a protocol for successful and efficient overexpression of the variants having Azk incorporated and the control expressions as mentioned above. The purification of small culture volumes below 400 mL must be optimized to obtain a concentration of protein that enables a determination of the specific enzyme activity with less Azk supply. The variants with the incorporated ncAA will have to be verified through mass spectroscopy. Following up, the three different variants of each model enzyme must

be assessed by their specific enzyme activity. The decrease of specific enzyme activity through the incorporation of the ncAA should be kept minimal. The variants displaying highest specific enzyme activity are intended for further proceeding. This will include light-driven biotransformations with different free photosensitizers, as well as the SPAAC of the photosensitizer to the enzyme variants. The photosensitizer based on FMN, which will be linked to an octyne moiety will be synthesized. It is expected that the enzyme-photosensitizer complex will display a higher turnover frequency due to the fast regeneration of the enzyme-own flavin moiety carrying the photosensitizer in steric proximity. The enzyme-photosensitizer complex is expected to enable a more efficient light-driven biotransformation with fewer by-products. The ability to use visible light efficient in chemistry leads to a more “greener” chemistry. This would offer not only an improved atom efficiency, but would also provide an effective, environmentally friendly and sustainable approach compared to traditional chemistry [13,38].

5 MATERIALS AND METHODS

5.1 DEVICES AND CHEMICALS

In this thesis, standard laboratory devices were used for the experiments, except for the self-developed light reactor, described in 5.5.9. General chemicals and other compounds were obtained from Sigma-Aldrich Inc. (Vienna, Austria) or Carl Roth GmbH (Karlsruhe, Germany). Important chemicals and compounds are shown in Table 8.

Table 8: Table of specific chemicals and compounds used in this thesis.

chemicals	commercial source	CAS number
azidolysine (*Azk*)	Iris Biotech GmbH (Marktredwitz, Germany)	1167421-25-1 net
NADPH, tetrasodium	Roche Diagnostics GmbH (Vienna, Austria)	2646-71-1
catalase	Carl-Roth GmbH (Karlsruhe, Germany)	9001-05-2
ε-caprolactone	Sigma-Aldrich Inc. (Vienna, Austria)	502-44-3
dichloromethane	Carl-Roth GmbH (Karlsruhe, Germany)	75-09-2
ethanol	Chem-Lab NV (Zedelgem, Belgium)	64-17-5
N,N-dimethylformamide	Sigma-Aldrich Inc. (Vienna, Austria)	68-12-2
acetophenone		98-86-2
Ni Sepharose™	GE Healthcare (Solingen, Germany)	
kanamycin sulfate	Carl-Roth GmbH (Karlsruhe, Germany)	25389-94-0
fluorescein sodium salt	Sigma-Aldrich Inc. (Vienna, Austria)	518-47-8

dibenzylcyclooctyne-PEG_4-5/6-FMA	Jena Bioscience GmbH (Jena, Germany)
*Dpn*I	Thermo Fisher Scientific GmbH (Vienna, Austria)
Pfu DNA polymerase	Promega GmbH (Mannheim, Germany)
Phusion DNA polymerase	Thermo Fisher Scientific GmbH (Vienna, Austria)
dimethylsulfoxide	Thermo Fisher Scientific GmbH (Vienna, Austria)
PageRuler™	Thermo Fisher Scientific GmbH (Vienna, Austria)

5.2 BUFFERS AND SOLUTIONS

5.2.1 TAE BUFFER

TAE buffer was prepared by creating a 50 x TAE buffer which was diluted to 1 x for usage. The composition of 50 x TAE buffer is shown in Table 9.

Table 9: TAE buffer composition.

50 x TAE	1 x TAE final concentration
242 g Tris	40 mM
57.1 mL glacial acetic acid	20 mM
100 mL of EDTA (500 mM, pH 8.0)	1 mM
to a final volume of 1 L with *dd*H_2O	

5.2.2 LYSIS BUFFER FOR PROTEIN PURIFICATION

The lysis buffer was prepared by dissolving 0.6808g imidazole in the compounds shown in Table 10 and filled up with *dd*H_2O to 900 mL. The pH was adjusted to 7.2 with HCl (1 M) and filled up with *dd*H_2O to 1 L.

Table 10: Compounds dissolved in lysis buffer, wash buffer and elution buffer.

compound	concentration	volume [mL]
NaH_2PO_4	1 M	11.1
Na_2HPO_4	1 M	38.9
NaCl	5 M	30

The final concentrations of the components in the lysis buffer were 50 mM NaPi, 150 mM NaCl and 10 mM imidazole.

5.2.3 WASH BUFFER FOR PROTEIN PURIFICATION

The lysis buffer was prepared by dissolving 2.042 g imidazole in the lysis buffer (see 1.2.1, Table 10) and filled up with *dd*H_2O to 900 mL. The pH was adjusted to 7.2 with HCl (1 M) and filled up with *dd*H_2O to 1 L. The final concentrations of the components in the wash buffer were 50 mM NaPi, 150 mM NaCl and 30 mM imidazole.

5.2.4 ELUTION BUFFER FOR PROTEIN PURIFICATION

The lysis buffer was prepared by dissolving 34.04 g imidazole in the compounds shown in Table 10 and filled up with *dd*H_2O to 900 mL. The pH was adjusted to 7.2 with HCl (1 M) and filled up with *dd*H_2O to 1 L. The final concentrations of the components in the wash buffer were 50 mM NaPi, 150 mM NaCl and 500 mM imidazole.

5.2.5 KPI BUFFER

The KPi buffer with a pH of 6.5 used for YqjM was prepared by dissolving 1.32 g K_2HPO_4 (174.18 g/mol) and 2.37 g KH_2PO_4 in 0.5 L *dd*H_2O. The KPi buffer with a pH of 8.0, used for CHMO, was prepared by dissolving 4.06 g K_2HPO_4

(174.18 g/mol) and 0.23 g KH_2PO_4 in 0.5 L *dd*H_2O. The pH of each buffer was adjusted with HCl.

5.2.6 SDS BUFFER AND SOLUTIONS

The ready to use SDS ExpressPlus™ PAGE Gels 10x8 as well as the corresponding running buffer were obtained from GenScript®. The running buffer was dissolved in 1 L *dd*H_2O according to the instructions of the manual from GenScript®.

5.2.7 SDS STAINING SOLUTION

The SDS staining solution was prepared according to Table 11.

Table 11: Components for 1 L SDS-page staining solution.

component	total volume of 1 L
Coomassie Brilliant Blue G250	1 g
clacial acetic acid (conc.)	100 mL
ethanol	300 mL
ddH_2O	600 mL

5.2.8 SDS DESTAINING SOLUTION

The SDS destaining solution was prepared according to Table 12.

Table 12: Components for 1 L SDS-page distaining solution.

component	amount for 1 L
clacial acetic acid (conc.)	100 mL
ethanol	300 mL
ddH_2O	600 mL

5.2.9 GLYCEROL STOCK SOLUTION

Glycerol stock solution was prepared with a concentration of 60 % (*w*/*w*) glycerol in *dd*H_2O and autoclaved before use.

5.3 MICROBIOLOGICAL METHODS

5.3.1 STRAINS

Table 13: Strains used for molecular cloning and expression

strain	genotype	description	source
E. coli TOP10	F-mcrA Δ(mrr-hsdRMS-mcrBC) φ80(lacZ)ΔM15 ΔlacX74 recA1 araD139 Δ(araleu)7697 galU galK rpsL (StrR) endA1 nupG λ-	routine cloning	Thermo Fisher Scientific GmbH (Vienna, Austria)
E. coli Mach 1	F-φ80(lacZ)ΔM15 ΔlacX74 hsdR(rK-mK+) ΔrecA1398 endA1 tonA	routine cloning	Thermo Fisher Scientific GmbH (Vienna, Austria)
E. coli BL21 (DE3)	F- ompT hsdSB (rBmB-) gal dcm (DE3)	high-level expression of recombinant protein	Thermo Fisher Scientific GmbH (Vienna, Austria)

Chemically competent *E. coli* TOP10 and *E. coli* Mach 1 cells were used for transformation after routine cloning. Chemically competent *E. coli* BL21 (DE3) cells were used for high-level expression of recombinant proteins. Specifications of the strains are shown in Table 13.

5.3.2 LIQUID MEDIA

The LB medium was prepared by dissolving 16 g of ready-to-use LB medium in *dd*H_2O to a final concentration of 20 g/L and autoclaved. The ready to use LB medium was obtained from Carl-Roth GmbH (Karlsruhe, Germany).

The TB medium was prepared separately as medium stock and salt stock as seen in Table 14 with compounds obtained from Carl-Roth GmbH (Karlsruhe, Germany). After separate autoclavation, the ready to use TB medium was prepared by adding 0.1 L of TB salts to 0.9 L of TB medium stock.

Table 14: List of components used for TB medium preparation.

TB medium stock	TB medium salt stock
21.59 g yeast extract	125.41 g K_2HPO_4
10.81 g tryptone/peptone	23.17 g KH_2PO_4
4.52 g glycerine	0.9 L *dd*H_2O
0.9 L *dd*H_2O	-

For regeneration after transformation, LB-SOC medium was used. SOC medium was prepared in a 10 x stock as seen in Table 15 and filtrated sterile (pore size 0.20 µm). For further usage, SOC was diluted with LB medium to a 1 x LB-SOC.

Table 15: Components of 10 x SOC stock.

SOC (10 x) stock
0.093 g KCl
0.952 g $MgCl_2$
1.204 g $MgSO_4$
1.982 g glucose monohydrate
0.05 L *dd*H_2O

The M9 medium was prepared with the ingredients shown in Table 16. The 5x M9 salt stock was prepared by dissolving 34 g/L $NaHPO_4$, 15 g/L KH_2PO_4, 2.5 g/L NaCl and 5 g/L NH_4Cl in 1 L *dd*H_2O.

Table 16: M9 medium preparation. All ingredients were kept in sterile stocks and were autoclaved or filtered sterile (0.20 µm). Trace elements were received from acib Wiltschi group.

M9 medium	stock concentration	volume for 500 mL [mL]

5x M9 salt stock	-	100
$MgSO_4$	1 M	0.5
$CaCl_2$	1 mg/mL	0.5
thiamine	1 mg/mL	0.5
glucose	1 M	10
trace elements	-	62.5
kanamycin	40 mg/mL	0.5
amino acid solution in HCl	0.5 g/L (HCl 0.1M)	50
biotin	1 mg/mL	0.5
ddH_2O	-	to 500 mL

5.3.3 PLATED MEDIA

The kanamycin plates were prepared by dissolving LB medium to a concentration of 20 g/L and agar to a concentration of 15 g/L in *dd*H_2O to a final volume of 800 mL and autoclaved. After cooling, kanamycin was added to a final concentration of 40 µg/mL and the medium was poured into petri dishes.

5.3.4 OVER-NIGHT CULTURES

Over-night cultures (*ONC*) were prepared in 50 mL falcons to a culture volume of 10 mL in LB medium containing kanamycin to a final concentration of 40 µg/mL. Inoculation was done by picking a single colony with a sterile inoculation loop. The ONC was incubated over-night at 37 °C with vigorous shaking at 130 rpm.

5.3.5 GLYCEROL STOCK

Glycerol stocks were prepared by mixing 1 mL of an ONC with 1 mL of the glycerol stock solution (60 % (v/v)) to reach a final concentration of 30 % (v/v) glycerol. The glycerol stocks were stored in cryotubes at -20 °C. Glycerol stocks prepared in this experiment are shown in Table 17 below.

Table 17: List of glycerol stocks prepared.

strain	plasmid	insert	promotor	his-tag
E. coli BL21 (DE3)	pSCS_MmOp_CHMO_T7	CHMO	T7	C-term.
E. coli BL21 (DE3)	pSCS_MmOp_CHMO_T5	CHMO	T5	C-term.
E. coli BL21 (DE3)	pSCS_MmOp_CHMO_T7_AzkE127	CHMO	T7	C-term.
E. coli BL21 (DE3)	pSCS_MmOp_CHMO_T7_AzkN156	CHMO	T7	C-term.
E. coli BL21 (DE3)	pSCS_MmOp_CHMO_T7_AzkR389	CHMO	T7	C-term.
E. coli BL21 (DE3)	pET28a_CHMO	CHMO	T7	C-term.
E. coli BL21 (DE3)	pET28a_CHMO	CHMO	T7	N-term.
E. coli BL21 (DE3)	pSCS_MmOp_YqjM_T7	YqjM	T7	C-term.
E. coli BL21 (DE3)	pET28a_YqjM	YqjM	T7	N-term.

5.4 MOLECULAR BIOLOGICAL METHODS

5.4.1 PRIMERS

All primers were designed with the *in-silico* cloning software Geneious[g] and obtained from Integrated DNA Technologies Inc. (*IDT*). The melting temperature (T_M) was calculated by using the T_M-calculator of Thermo Fisher Scientific Gmbh (Vienna, Austria). Primers used for DNA amplification and DNA sequencing were designed with an average length of ~20-25 nucleotides (*nt*) and a T_M difference of not more than 5 °C. Primers used for different cloning strategies were designed with varying

T_M and length of nucleotides according to the cloning strategy. To introduce a T7 promotor upstream the GOI, a primer with a length of 116 nt was used. A list of all used primers can be found in the Appendix under 7.1 List of primers.

5.4.2 PLASMIDS

The vector pSCS_MmOp which was provided by the acib (Austrian Centre of Industrial Biotechnology by Birgit Wiltschi [28]) was used in this thesis. This vector served as the backbone for generating all wildtype plasmids. Furthermore, the commercial cloning vector pET28a was used for GOI recovery and comparison. All plasmid constructs generated during this thesis can be seen in Table 18.

Table 18: List of all plasmids used in this thesis. All plasmids carry a kanamycin resistance.

plasmid	insert	promotor	his-tag	MOD
pSCS_MmOp	GFP	T5	N-term.	
pSCS_MmOp_CHMO_T7	CHMO	T7	C-term.	
pSCS_MmOp_CHMO_T5	CHMO	T5	C-term.	
pSCS_MmOp_CHMO_T7_AzkE127	CHMO	T7	C-term.	Azk E127
pSCS_MmOp_CHMO_T7_AzkN156	CHMO	T7	C-term.	Azk N156
pSCS_MmOp_CHMO_T7_AzkR389	CHMO	T7	C-term.	Azk R389
pET28a_CHMO	CHMO	T7	C-term.	
pET28a_CHMO	CHMO	T7	N-term.	
pSCS_MmOp_YqjM_T7	YqjM	T7	C-term.	
pSCS_MmOp_YqjM_T7_AzkT70	YqjM	T7	C-term.	AzkT70
pSCS_MmOp_YqjM_T7_AzkK109	YqjM	T7	C-term.	AzkK109
pSCS_MmOp_YqjM_T7_AzkE335	YqjM	T7	C-term.	AzkE335
pET28a_YqjM	YqjM	T7	N-term.	

5.4.3 IN-SILICO CLONING

For in-silico cloning and experiment design, the program Geneious[g] was used to design the molecular cloning experiments and strategies. Geneious[g] was used as well for evaluation of sequencing data received from Microsynth AG (Balgach, Switzerland).

5.4.4 RESTRICTION/LIGATION

For ligation, the vector and the amplified insert, encoding for the GOI, were digested with *Bgl*II and *Nde*I for 2.5 hours at 37 °C. The enzymes were inactivated at 80 °C for 10 minutes. The vector was separated by a preparative 1 % (w/v) agarose gel and the respective band was excised and cleaned with the Wizard SV Gel and PCR Clean-up, provided by Promega GmbH (Mannheim, Germany). The vector and insert were ligated as shown in Table 19.

Table 19: Components of a restriction-ligation reaction.

component	volume [µL]
vector [80 ng]	4
insert [240 ng]	4
10 x T4 ligase buffer	1
T4 ligase	0.5
ddH_2O	0.5

The ligation reaction was incubated at 16 °C for 16 hours. The ligation reaction was inactivated by incubation at 70 °C for 20 minutes. *E. coli* Mach1 cells were transformed with 3 µL of the ligation mix, streaked out on LB-KAN plates and incubated over-night at 37 °C. For validation of successful transformed *E. coli* Mach1 cells with the ligated construct, a colony PCR was performed, and the hits were sequenced.

5.4.5 GIBSON ASSEMBLY®

Gibson assembly® is a method for rapid cloning by one-pot *in vitro* recombination. This method is based on linearized DNA fragments which are recombined by their

homologous regions. The Gibson mix contains a T5 exonuclease, a Phusion DNA polymerase and Taq DNA ligase in the corresponding buffer. The reaction was performed in a volume of 7.5 µL Gibson mix and 2.5 µL of DNA fragments, vector and insert, at 50 °C for 60 minutes. Afterwards, chemo-competent *E. coli* Top10 cells were transformed with the Gibson assembly® product. The cells were regenerated in 1 x LB-SOC medium for 1 hour at 37 °C, afterwards plated onto LB-kanamycin (40 µg/mL) plates and incubated over-night at 37 °C.

5.4.6 FAST CLONING

Fast cloning is a PCR cloning method suitable for cloning DNA fragments into vectors at any desired position. For this method neither restriction nor ligation enzymes are necessary. Four primers were designed, whereby two primers are always complementary. These primers should be complementary at around 15 bases of the GOI and 15 of the vector of interest and should end with guanine or cytosine as shown in Figure 21.

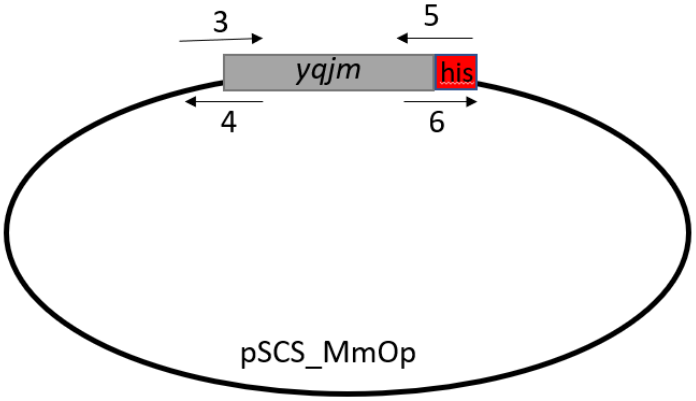

Figure 21: Fast cloning of *yqjm* into the pSCS_MmOp vector. Arrows show the position of the Primers used, Primer 3 and 5 were used to amplify the GOI, the primers 4 and 6 were used for amplification of the vector pSCS_MmOp.

Two separate regular PCRs were performed to amplify vector and the GOI, creating the complementary sequences to each other. Afterwards, 45 µL of each PCR product was digested with 0.5 µL *Dpn*I for 120 minutes. The reaction was stopped by incubating at 80 °C for 10 minutes, and the vector and a respective amount (1:3) of the insert were combined. Chemically competent *E. coli* Top10 cells were then transformed with 3 µL cloning product.

5.4.7 QUIKCHANGE™

QuikChange™ is a method for site-directed mutagenesis. The primers were designed to be complementary for the first third, introducing the mutation, and not complementary for the rest of the sequence, to prevent primer self-annealing (Figure 22).

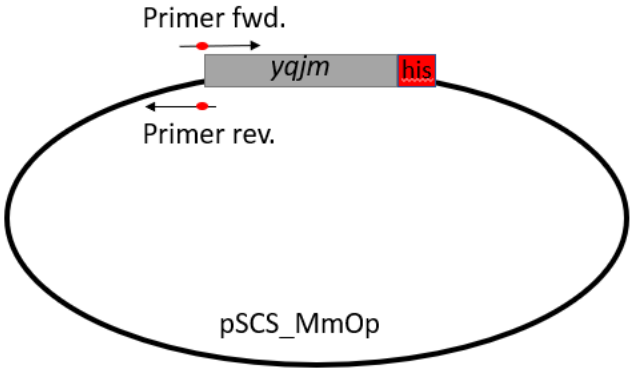

Figure 22: Primer design for the QuikChange™ method. Arrows indicating the primers. The red dot marks the position of the mutation.

For the actual QuikChange™ reaction (Table 20), a temperature gradient program (Table 21) was performed.

Table 20: QuikChange™ reaction mix used for site-directed mutagenesis.

QuikChange™	8x 20 [µL]
ddH_2O	132.4
10x Pfu buffer	16
forward Primer (10 µM)	2
reverse Primer (10 µM)	2
dNTPs (10 mM)	4
template (100 ng/µL)	2
DMSO (100 %)	0.8
Pfu polymerase	0.8

Table 21: Gradient program for QuikChange™ method.

QuikChange™ program	temperature [°C]	time [min]	cycles
heating	95	1	
denaturation	95	0.5	
annealing	45-72	0.5	x 20
elongation	72	7	
final elongation	72	10	
hold	4	∞	

5 µL of each QuikChange™ reaction was analyzed with a 1 % (w/v) agarose gel. The remaining PCR product was digested with 1 µL *Dpn*I for 120 minutes at 37 °C. The digestion was stopped by incubating at 80 °C for 20 minutes. *E. coli* Top10 cells were transformed with 3 µL of the QuikChange™ product.

5.4.8 TRANSFORMATION OF CHEMICALLY COMPETENT *E. COLI* CELLS

The transformation was performed with chemically competent *E. coli* TOP10 cells, chemically competent *E. coli* BL21 (DE3) or chemically competent *E. coli* Mach 1 cells. To 50 µL of ice-thawed chemo-competent cells, 1-5 µL of plasmid DNA was added and incubated for 30 min on ice. A heat shock at 42 °C for 42 seconds was performed followed by addition 300-400 µL LB-SOC medium for regeneration. The cells were regenerated at 37 °C and 350 rpm for 1 hour. Afterwards, the cells were plated onto LB-kanamycin plates and incubated at 37 °C overnight.

Before expression, the confirmed plasmid of interest was isolated from *E. coli* TOP10 or *E. coli* Mach1, and 5 µL of plasmid were retransformed into *E. coli* BL21 (DE3).

5.4.9 PLASMID ISOLATION

Plasmid isolations were either performed with the Wizard® Plus SC Miniprep DNA Purification System from Promega GmbH (Mannheim, Germany) or with GeneJet Plasmid Miniprep kit from Thermo Fisher Scientific GmbH (Vienna, Austria). Both methods were performed according to the manufacturer's instructions. The methods

are based on the lysis of the cells. After neutralization, the plasmid DNA precipitates onto a minicolumn. After washing steps, the plasmids were eluted with 50 µL *dd*H_2O.

5.4.10 RESTRICTION ANALYSIS

The restriction analysis was performed with two FastDigest enzymes provided by Thermo Fisher Scientific GmbH (Vienna, Austria). The digestion was first done *in silico* in order to predict the length of the digested DNA fragments. The restriction, as shown in Table 22, was performed in a volume of 20 µL directly with the isolated plasmid.

Table 22: Restriction digestion of a plasmid.

restriction	volume [µL]
plasmid	16
Fast digest green buffer x10 (Thermo Fisher Scientific GmbH, Vienna, Austria)	2
restriction enzyme 1 (*Nde*I)	1
restriction enzyme 2 (*Bgl*II)	1

After incubating the mix for 1.5 hours at 37 °C, the samples were directly loaded onto a 1 % (w/v) agarose gel.

5.4.11 POLYMERASE CHAIN REACTION - GENERAL

In this thesis, all PCRs were performed in a Bio-Center GE4852T™ PCR-cycler. Polymerase chain reactions (*PCR*) were prepared in a master mix which is shown in Table 23. In general, the master mix included a DNA polymerase, the suitable buffer, a forward and a reverse primer, nucleotides as well as a DNA template. The reaction volumes of a single PCR typically were 20 µL or 50 µL. The polymerase was chosen according to the experimental needs due to the error rates and proofreading function of a certain polymerase in order to produce stringent results.

Table 23: General set-up of a polymerase chain reaction.

PCR	final concentration
ddH_2O	100 %
polymerase buffer	x 1
forward primer	10 µM
reverse primer	10 µM
dNTPs (10 mM)	2 mM
template vector	0.5 ng/µL
DNA polymerase	5 U/µL

The PCR program is shown in Table 24. The number of repetitions was chosen in respect to the DNA template, the used polymerase and the amount of amplified DNA needed.

Table 24: Polymerase chain reaction thermocycler program.

PCR program	temperature [°C]	time [min]	cycles
initial heating	95	1	
denaturation	95	0.5	
annealing	53	0.5	x 20-30
elongation	72	0.5-1 (per 1 kb)	
final elongation	72	7-10	
hold	4	∞	

5.4.12 Gradient polymerase chain reaction

Gradient PCR was done in case a normal PCR did not or only to a small extent lead to amplified DNA. Therefore, 6 different annealing temperatures were chosen in the reaction. This increases the possibility to identify the optimal annealing temperature. These temperatures were chosen in a first approach to be in a range of 5 °C lower and higher than the calculated T_M (Thermo Fisher Scientific GmbH (Vienna, Austria)

T_M calculator). If no positive results were obtained, the T_M was chosen to be lower, but not below 45 °C.

5.4.13 COLONY POLYMERASE CHAIN REACTION

A colony polymerase chain reaction (cPCR), performed in a Bio-Center GE4852T™ PCR-cycler, is characterized by using whole-cell material as a template. To extract the DNA template for the PCR from the *E. coli* cells, the initial heating of the PCR program is expanded. A One Taq Quick Load x 2 Master mix was used for colony PCRs performed in a reaction volume of 10 µL, as shown in Table 25.

Table 25: Set up of a colony polymerase chain reaction

cPCR	1 x 10 [µL]
ddH_2O	4.6
One Taq Quick Load x2 master mix	5
primer 11	0.2
primer 12	0.2
single colony cell material	-

For inoculation of 10 µL PCR, a small amount of cell material was picked. After PCR the PCR mix was directly loaded onto a 1 % (w/v) agarose gel.

5.4.14 AGAROSE GEL ELECTROPHORESIS

A 1 % (*w/v*) agarose gel containing 0.002 % (v/v) ethidium bromide was used for detection of DNA fragments. The gel was prepared by dissolving 2 g of agarose in 200 mL 1 x TAE buffer. After dissolving, 4 µL ethidium bromide were added for visualization, poured into prepared gel moulds and cooled. Before loading, 5 µL of the sample was mixed with 1 µL of 6 x loading dye. To determine the size, the standard Generuler® 1 kb DNA Ladder (Thermo Fisher Scientific GmbH, Vienna, Austria) was applied.

If recovery of the desired DNA fragment after agarose gel electrophoresis was necessary, a preparative gel was prepared by creating larger slots suitable to carry up to 200 µL sample. Samples were prepared with 6 x loading dye to a final

concentration of 1 x loading dye. The respective bands were recovered from the gel by cutting the gel.

The settings chosen to run the agarose gel electrophoresis were 140 V for 40 minutes at a BioRad PowerPac™ Basic power supply. The detection was done with UV irradiation by using GelDoc-It™ Imaging system using the analysis software Launch VisionWorksLS.

5.4.15 GEL EXTRACTION

The recovery of DNA fragments from agarose gel electrophoresis was performed by using purification kits. Used systems were either the Wizard® SV Gel and PCR Clean-up System from Promega GmbH (Mannheim, Germany), or the GeneJET Gel Extraction Kit from Thermo Fisher Scientific GmbH (Vienna, Austria). Both systems, based on mini-column precipitation, were executed according to the manufacturer's instructions.

5.4.16 DNA SEQUENCING

Validation of the plasmid sequence was done by sequencing the plasmid isolate via Sanger Sequencing performed by Microsynth AG (Balgach, Switzerland). Primers for sequencing were provided beforehand, shown in the Appendix under 7.1 List of primers, or synthesized by the company.

5.5 BIOCHEMICAL METHODS

5.5.1 HETEROLOGOUS EXPRESSION OF RECOMBINANT PROTEIN

EXPRESSION IN 400 mL

An ONC was prepared by inoculating 10 mL LB medium containing kanamycin to a final concentration of 40 µg/mL with the expression strain and incubated over-night at 37 °C in a shaker at 130 rpm. The main culture was prepared in TB medium with kanamycin (40 µg/mL) and inoculated to an OD_{600} of 0.1. The OD_{600} was monitored until an OD_{600} of 0.6 to 0.8 was reached for induction. After taking a sample, the main culture was induced with IPTG (stock 1 M) to a final concentration of 0.1 mM. For expression, the main culture was incubated at 20 °C over-night at 130 rpm under vigorous shaking.

The cells were harvested by centrifugation at 4000 rpm for 15 minutes and the supernatant was discarded. The pellet was washed with 20 mL of 0.9 % NaCl, centrifuged at 4000 rpm for 15 minutes and the supernatant was discarded. The pellet further proceeded immediately for cell disruption.

EXPRESSION IN 30 mL

The ONC (kanamycin 40 µg/mL) was used to inoculate the main culture of 30 mL TB medium (kanamycin; 40 µg/mL) with *E. coli* BL21 (DE3), carrying the respective plasmid, to an OD_{600} of 0.1. Induction was performed at an OD_{600} of 0.6 to 0.8 after taking a sample. The main culture was induced with IPTG (stock 1 M) to a final concentration of 0.1 mM. The main culture was incubated overnight at 20 °C under vigorous shaking (130 rpm).

The cells were harvested by centrifugation at 4.000 rpm for 15 minutes. Then the pellet was washed with 2 mL of 0.9 % NaCl and centrifuged again at 4.000 rpm for 15 minutes. The supernatant was discarded, and the pellet proceeded immediately for cell disruption.

5.5.2 HETEROLOGOUS EXPRESSION OF RECOMBINANT PROTEIN WITH AZK

Heterologous expression of recombinant CHMO variants carrying an AMBER stop codon was performed as mentioned in 5.5.1. Transcription of the GOI was induced with IPTG, whereas the transcription of the gene encoding the tRNA was induced with arabinose. Azidolysine was added to the main culture at the point of induction. All concentrations are shown in Table 26.

Table 26: Compounds needed for heterologous expression of CHMO variants carrying an AMBER stop codon.

compound	stock concentration	final concentration
IPTG	1 M	0.1 mM
arabinose	20 %	0.2 %
azidolysine	-	5 mM

5.5.3 PROTEIN PURIFICATION

Protein purification was performed with Ni Sepharose™ 6 Fast Flow provided by GE Healthcare (Solingen, Germany).

PROTEIN PURIFICATION IN 1.5 mL REACTION TUBE

Ni Sepharose™ was used, and all centrifugations were carried out with a tabletop centrifuge, using 1.5 mL reaction tubes at 13.200 rpm for 1 minute. 300 µL of Ni Sepharose™ were transferred into a 1.5 mL reaction tube and centrifuged. The supernatant was discarded. The Ni Sepharose™ was washed by adding 250 µL wash buffer (300 mM imidazole), then centrifuged and the supernatant was discarded. This step was repeated once. 800 µL of the cell-free extract was added to the Ni Sepharose™ and incubated on ice for 30 minutes while regularly inverting the reaction tube. After centrifugation, the supernatant was collected as the first fraction after loading the protein onto the beads. 250 µL of wash buffer (300 mM imidazole) was added to the reaction tube and centrifuged afterwards. The supernatant was collected as wash fraction. This step was repeated three times. For elution, 200 µL of elution buffer (300 mM imidazole, see section 5.2.4) were added and incubated for 1 minute. After centrifugation, the supernatant was collected to obtain the elution fraction. This step was repeated twice. After washing the Ni Sepharose™ with 200 µL of elution buffer (500 mM imidazole) and twice with 200 µL of wash buffer (30 mM imidazole), the Ni Sepharose™ was stored in the fridge (4 °C) as well as all samples, taken while protein purification, for further use.

PURIFICATION WITH 24 mL COLUMN VOLUME

2 mL of Ni Sepharose™ were inserted into a column as carrier material. After the ethanol of the Ni Sepharose™ ran through, the column was washed once with 7 mL *dd*H_2O and twice with 7 mL wash buffer (30 mM imidazole). The cell-free extract form protein expression was loaded onto the column and incubated on ice for 30 minutes while shaking at 4 °C. After incubation, the run-through was collected, and the column was washed four times with 7 mL wash buffer (30 mM imidazole). Each wash fraction was collected. For elution 1 mL of elution buffer with an imidazole concentration of 300 mM was applied onto the Ni Sepharose™, incubated for 1 minute and the elution was collected and stored on ice. This was repeated for three times. The protein of interest was recovered in the first 3 mL of elution. 6 mL

of elution buffer (300 mM imidazole) were applied and the flow-through was collected. For elution of all protein, another 10 mL of elution buffer containing 500 mM imidazole were applied. After washing the column again with wash buffer (30 mM imidazole), the column was stored in 4 mL of 20 % ethanol in the fridge.

5.5.4 PROTEIN DESALTING

The PD-10 columns were used according to the manufacturer's manual. After cutting the tip off and discarding excess liquid, the column was equilibrated with KPi Buffer (pH 6.5). 2.5 mL of elution fraction was loaded onto the column and the run-through was discarded. For elution 3.5 mL of KPi buffer (pH 6.5) was used and the flow-through collected.

5.5.5 PROTEIN CONCENTRATING

Samples were concentrated if needed by using the Vivaspin20 columns from GE Healthcare (Solingen, Germany), with a 10.000 MWCO PES membrane, and were used according to the manual.

5.5.6 PIERCE™ BCA PROTEIN ASSAY KIT

According to the instructions of the provider, Thermo Fisher Scientific GmbH (Vienna, Austria), the albumin standard dilutions of concentration from 0 µL/mL up to 2000 µL/mL of albumin were established. The working reagent was prepared according to the manual. For reaction, 25 µL of each standard or sample was pipetted in triplicates into the 96 well microplate. Afterwards, 200 µL of working reagent was added and the plate was incubated at 37 °C for 30 minutes. The absorbance of the samples has been measured at 562 nm by an Eon™ BioTek™ plate reader.

5.5.7 SDS-PAGE

For SDS-PAGE the ready to use ExpressPlus™ PAGE Gels from GenScript were used. The samples for the SDS-PAGE were prepared to a final volume of 20 µL by transferring 15 µL of a sample into a new reaction tube and adding 5 µL of SDS sample buffer. Afterwards the samples were incubated for 10 minutes at 95 °C and then loaded onto the SDS page. The settings of the power supply have been adjusted to 140 V and 75 mA for 65 minutes chosen according to the manual of the

producer. The SDS gel was stained with a staining solution (see section 5.2.7) for 1 hour and destained with a destaining solution (see section 5.2.8) for 2 hours.

5.5.8 NADPH ACTIVITY ASSAY

NADPH activity assay was performed to determine the initial specific enzyme activity of the model enzymes CHMO and YqjM. The standard reactions are shown in Table 27 and

Table 28.

Table 27:Standard reaction for NADPH activity assay for determination of the initial specific enzyme activity of YqjM. For YqjM a KPi buffer with pH 6.5 and cyclohexenone as substrate. The reaction was performed in a final volume of 1 mL in a cuvette.

compound	final concentration
KPi buffer (pH 6.5)	
glucose	20 mM
glucose oxidase	10 U/mL
NADPH	0.3 mM
cyclohexenone	1 mM
purified YqjM	1-10 µL/mL

Table 28:Standard reaction for NADPH activity assay for determination of the initial specific enzyme activity of CHMO. For CHMO a KPi buffer with pH 8 and cyclohexanone as substrate. The reaction was performed in a final volume of 1 mL in a cuvette.

compound	final concentration
KPi buffer (pH 8)	
NADPH	0.3 mM
cyclohexanone	1 mM
purified CHMO	1-10 µL/mL

The detection was performed using Cary 100 UV-Vis spectrophotometer by Agilent Technologies.

5.5.9 CONSTRUCTION OF LIGHT REACTOR

Due to the lack of a proper reactor for light-driven biotransformations without relevant heat build-up, a new concept was created by Dipl.-Biochem. Dr.rer.nat. Sandy Schmid and Michael Runda, BSc. Previous experiments showed the problem of heat dissipation because even LED lamps potentially produce enough heat to adulterate the results. The material needed to built-up a new light reactor is shown in Table 29 and was obtained from a regular hardware store.

Table 29: Material needed to build a reactor for light-driven biotransformations.

supply	measurements/details
1 x wooden board	70 cm x 30 cm
2 x acrylic glass panels	70 cm x 30 cm
6 x small case legs	6 cm x 6 cm x 10 cm
6 x threaded rods	25 cm – 30 cm, 10 mm
18 x nuts and flat washers	Suitable for the threaded rods
3 x light source (as much lumen and little heat as possible, preferably LED).	64 cm x 5 cm x 3 cm
24 x small screws with nuts and flat washers	To anchor the legs and the threaded rods, 4x30 mm
1 x electric wiring	with ON/OFF switch and electrical plug
consumables	screw joints, zip ties, terminal strips etc.

Main tools used were a circular saw, a drill press, a grinder bench, a soldering iron, cordless drill with Forstner bits, and a metal saw.

The wooden board and the acrylic glass panels were cut with a circular saw to the right measurements (Table 29). Holes for the threaded rods were drilled with a 12 mm diameter drill bit into the desired positions at the reactor. The threaded rods were stabilized by small case legs which were as well as the light sources mounted onto the wooden base. After assembling the electric wiring of the light sources, the

light reactor was assembled as seen in Figure 23. For inserting reaction vials into the light reactor, the upper acrylic glass panel was provided with holes with a diameter of 3 cm for 12 mL GC vials. In this experiment, a final reaction volume of 2 mL was used.

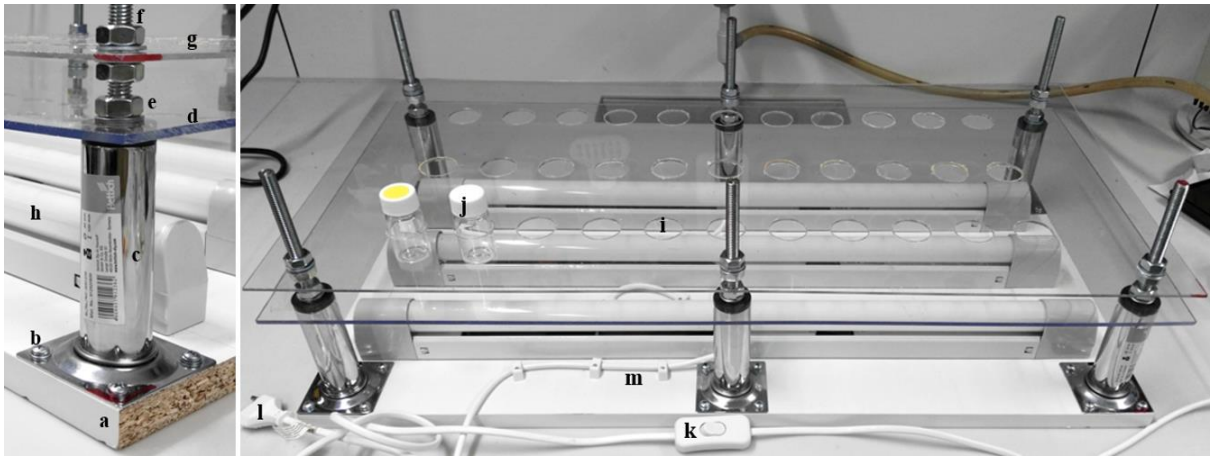

Figure 23: Setup of the light reactor: wooden board (a), screws and flat washers (b), case leg (c), acrylic glass panels (d, g), nuts with flat washers (e), threaded rod (f), light source (h), holes for vials (i), reaction vials (j), ON/OFF switch (k), electric plug (l) electrical wiring (m).

Dark reactions were performed in the light reactor by wrapping the samples in two layers of aluminium foil. Additionally, conventional LED strips were mounted onto the middle acrylic glass panels and used instead of the installed light source, when blue light was used for the biotransformation.

5.5.10 LIGHT-DRIVEN BIOTRANSFORMATIONS

Light-driven biotransformations were performed in a reaction volume of 2 mL in 20 mL screw-capped glass vials. Samples of 500 µL were taken after 0 hours and 24 hours for each reaction. The standard reaction setup is shown in Table 30.

Table 30: Light-driven biotransformation standard reaction setup.

reaction compounds	stock concentration	final concentration
KPi buffer pH 8.0	-	-
EDTA	280.9 mM	50 mM
cyclohexanone	50 mM	10 mM
FMN/fluorescein/FAD	10 mM	100 µM

CHMO	-	50 µM

Reactions can be seen in Table 31. As for the positive control, a reaction using NADPH was performed in KPi buffer pH 8.0 with 10 mM cyclohexanone and 50 µM CHMO.

Table 31: Different reaction setups for light-driven biotransformation.

	standard reaction	light	CHMO	FMN	fluorescein	FAD
1	FMN reaction	X	X	X		
2	FMN reaction		X	X		
3	fluorescein reaction	X	X		X	
4	fluorescein reaction		X		X	
5	FAD reaction	X	X			X
6	FAD reaction		X			X
7	enzyme blank A	X		X		
8	enzyme blank B	X			X	
9	FMN/fluorescein/FAD blank	X	X			
10	NADPH reaction		X			

5.5.11 ORGANIC PHASE EXTRACTION

Organic phase extraction was performed with dichloromethane containing 2 mM acetophenone as internal standard (DCM-Ap). 500 µL sample, taken from the biotransformations, was mixed with 500 µL of DCM-Ap and vigorous shook for 1 minute. Afterwards, the sample was centrifuged for 1 minute at 13.200 rpm. The lower organic phase was transferred into a new 1.5 mL reaction tube containing a spatula tip of $MgSO_4$. After vigorous shaking for 3 seconds, the sample was centrifuged for 10 minutes at 13.200 rpm. 200 µL of sample was transferred into a 2 mL GC-vial for analyzes.

5.5.12 GAS CHROMATOGRAPHY-FLAME IONIZATION/MASS SPECTROMETRY

A Shimadzu Nexis GC-2030 equipped with a β-Hydrodex-3P column was used for the chiral quantitative analysis. A method was established to enable the GC-FID to detect the substrate cyclohexanone and product ε-caprolactone in one method. All parameters for GC-FID analysis are shown in Table 32.

Table 32: GC-FID parameters used for detection of cyclohexanone and ε-caprolactone.

GC-FID parameters	
instrument	Shimadzu Nexis GC-2030
column	ß-Hydrodex-3P; film thickness 0.25 µm, column length 50.0 m, inner diameter 0.25 mm, column max. temperature 220.0 °C
injection volume	1.0 µL
injection temp.	230.0 °C
injection mode	split
flow control mode	velocity
pressure	173.0 kPa
total flow	174.7 mL/min
column flow	1.70 mL/min
linear velocity	32.6 cm/s
purge flow	3.0 mL/min
split ratio	100.0
oven temp. program	3.0 min 60.0 °C 10.0 °C/min to 220.0 °C for 31.0 min
FID temperature	250.0 °C

The calibration curve for chiral quantitative analysis using GC-FID was generated by setting up samples of DCM containing 2 mM acetophenone and cyclohexanone (Figure 24) or ε-caprolactone (Figure 25) at a concentration range of 0.1 mM to

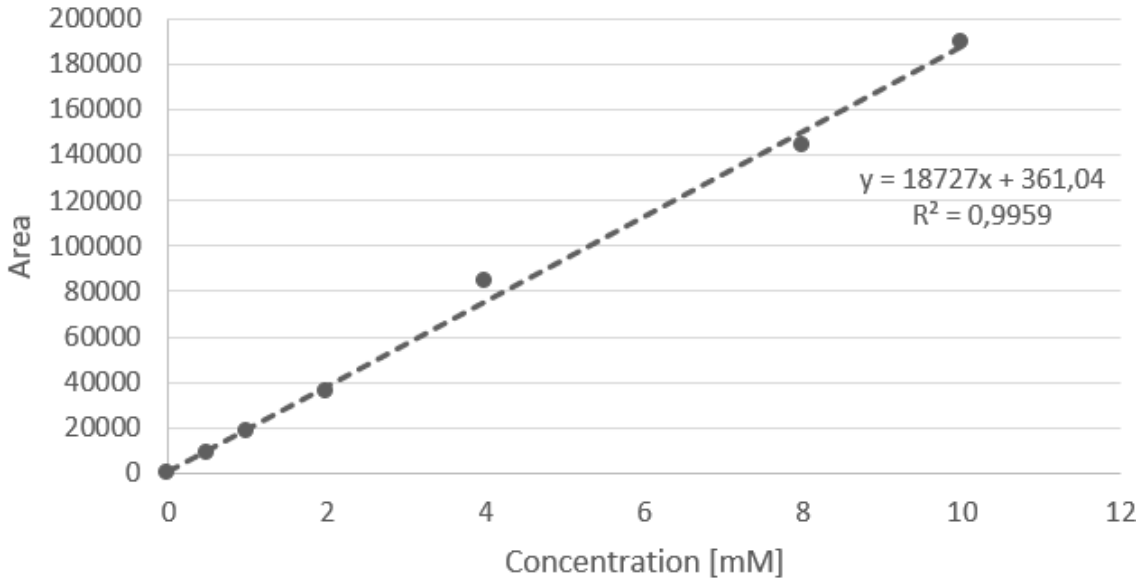

10 mM.

Figure 24: Calibration curve of cyclohexanone.

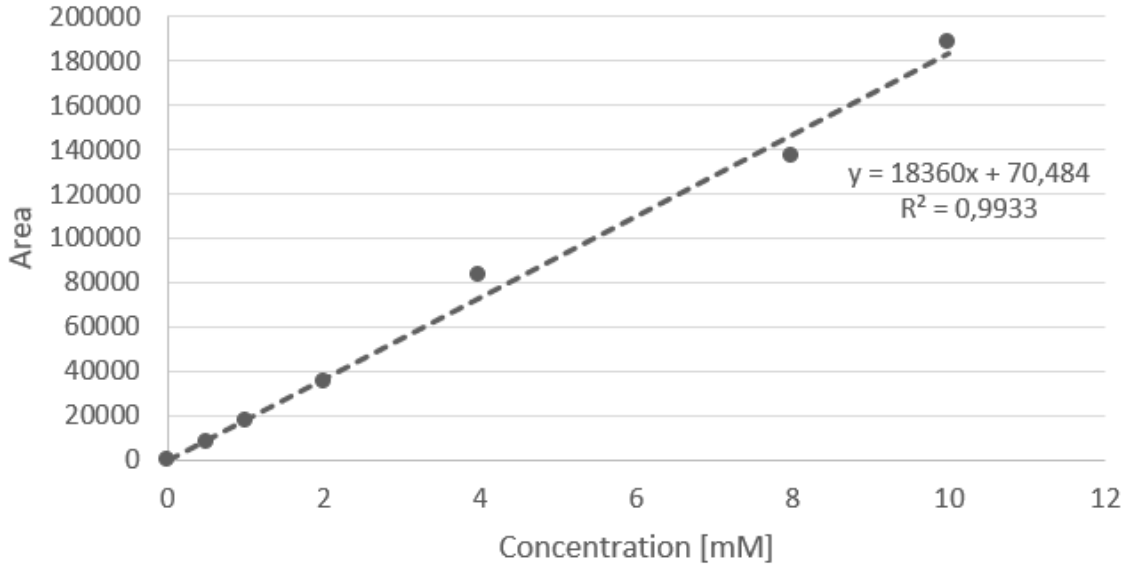

Figure 25: Calibration curve of ε-caprolactone.

5.5.13 STRAIN-PROMOTED AZIDE-ALKYNE CYCLOADDITION

Copper-catalyzed alkyne azide cycloaddition, as one of the most popular methods of cycloaddition, it suffers from major drawbacks. Copper, a toxic transition metal, negatively influences enzyme stability and activity. Moreover, the removal of copper,

for example by dialysis, can be problematic[18,23,24]. A copper-free cycloaddition based on a cycloaddition of cyclooctyne with phenylazide leading to the corresponding triazole was investigated. Strain-promoted azide-alkyne cycloaddition is used for labelling peptides [18].

For the preservation of the enzyme properties, strain-promoted azide-alkyne cycloaddition was used. SPAAC is based on the exothermic cycloaddition of cyclooctyne with phenyl azide leading to a triazole and offers a broad biorthogonal chemical spectrum of application [18]. The SPAAC was performed with the CHMO variant carrying Azk at position N156 and the clickable photosensitizer dibenzylcyclooctyne-PEG$_4$-5/6-FMA (*DBCO-PEG$_4$-5/6-FMA;* Jena Bioscience GmbH (Jena, Germany Figure 26).

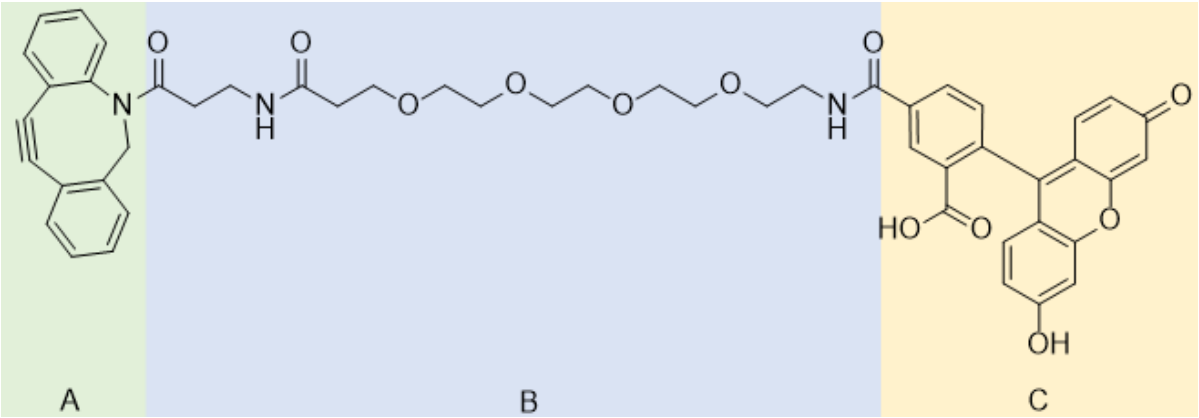

Figure 26: Dibenzylcyclooctyne-PEG$_4$-5/6-FMA, provided by Jena Bioscience GmbH (Jena, Germany), consists of an octyne moiety (A) connected by an ether linker (B) to fluorescein (C) serving as a photosensitizer.

The DBCO-PEG$_4$-5/6-FMA (molecular weight: 881.32 g/mol) was fully dissolved in 200 µL DMF leading to a concentration of 5675 µM. 2 µL of the dissolved DBCO-PEG$_4$-5/6-FMA was added to 150 µL of CHMO variant N156 to get an equimolar concentration of photosensitizer and protein of 75 µM. The click reaction was performed over-night at 22 °C. The mixture was then desalted twice with a PD MiniTrap^{TM} G-10 (GE Healthcare (Solingen, Germany)), as described previously in 5.5.4 protein desalting, and detection was performed by spectroscopy.

5.5.14 Spectroscopic detection of Photozyme

The spectroscopic detection of the *Photozyme* was performed by measuring the fluorescence of the photosensitizer. The spectroscopic properties of DBCO-PEG$_4$-5/6-FMA are λ_{exc} 492 nm and λ_{em} 517 nm with a □83.0 L/mmol*cm after click

reaction. The detection was performed with the BMG POLARstar galaxy photometer using a black microtiter plate having KPi buffer pH 8 as blank. CHMO without DBCO-PEG$_4$-5/6-FMA was used as a standard and samples, taken from copper-free azide-alkyne cycloaddition reaction after first desalting and after second desalting, were spectroscopically measured. All measurements were performed in triplicates.

5.6 Biophysical Methods

5.6.1 Cell disruption

For the disruption of the cells, the pellet obtained by heterologous expression in 400 mL culture volume, was dissolved in 25 mL lysis buffer and sonicated twice for 3 minutes on ice with a duty cycle of 50 %, output control of 5 and micro tip limit of 5. The cell extract was transferred into 40 mL centrifugation tubes. After centrifugation at 4 °C and 20.000 rpm for 40 minutes, the supernatant was sterile filtered (pore size 0.45 µm) and used for protein purification.

For the disruption of the cells, the pellet obtained by heterologous expression in 30 mL culture volume, was dissolved in 2 mL lysis buffer and sonicated twice for 30 seconds on ice with a duty cycle of 50 %, output control of 5 and micro tip limit of 5. The disrupted cells were transferred into 1.5 mL centrifugation tube. After centrifugation at 4 °C and 13.200 rpm for 20 minutes, the supernatant was used for protein purification, without sterile filtration to prevent loss of supernatant.

6 REFERENCES

1. Tucker, J.L. (2006) Green chemistry, a pharmaceutical perspective. *Org. Process Res. Dev.*, **10** (2), 315–319.

2. D. Gamenara, G. A. Seonane , P. Saenz-Mendez, P.D. de M. (2013) *REDOX BIOCATALYSIS Fundamentals and Applications*.

3. Martínez, A.T., Ruiz-Dueñas, F.J., Camarero, S., et al. (2017) Oxidoreductases on their way to industrial biotransformations. *Biotechnol. Adv.*, **35** (6), 815–831.

4. Dong, J.J., Fernández-Fueyo, E., Hollmann, F., Paul, C.E., Pesic, M., Schmidt, S., Wang, Y., Younes, S., and Zhang, W. (2018) Biocatalytic Oxidation Reactions: A Chemist's Perspective. *Angew. Chemie - Int. Ed.*, **57** (30), 9238–9261.

5. Kourist, R., Domínguez De María, P., and Miyamoto, K. (2011) Biocatalytic strategies for the asymmetric synthesis of profens - Recent trends and developments. *Green Chem.*, **13** (10), 2607–2618.

6. Sheng, D., Ballou, D.P., and Massey, V. (2001) Mechanistic studies of cyclohexanone monooxygenase: Chemical properties of intermediates involved in catalysis. *Biochemistry*, **40** (37), 11156–11167.

7. Toogood, H.S., and Scrutton, N.S. (2018) Discovery, Characterization, Engineering, and Applications of Ene-Reductases for Industrial Biocatalysis. *ACS Catal.*, **8** (4), 3532–3549.

8. Lee, S.H., Choi, D.S., Pesic, M., Lee, Y.W., Paul, C.E., Hollmann, F., and Park, C.B. (2017) Cofactor-Free, Direct Photoactivation of Enoate Reductases for the Asymmetric Reduction of C=C Bonds. *Angew. Chemie - Int. Ed.*, **56** (30), 8681–8685.

9. Knaus, T., Toogood, H.S., and Scrutton, N.S. (2016) *Ene-reductases and their Applications*. Green Biocatalysis, First Edition, John Wiley & Sons, Inc.

10. Doran, P.M. (2013) *ENGINEERING PRINCIPLES SECOND EDITION*. Elsevier Ltd.

11. Cantó, C., Menzies, K.J., and Auwerx, J. (2015) NAD+ Metabolism and the Control of Energy Homeostasis: A Balancing Act between Mitochondria and the Nucleus. *Cell Metab.*, **22** (1), 31–53.

12. Schmidt, S., Scherkus, C., Muschiol, J., Menyes, U., Winkler, T., Hummel, W., Gröger, H., Liese, A., Herz, H.G., and Bornscheuer, U.T. (2015) An enzyme cascade synthesis of ε-caprolactone and its oligomers. *Angew. Chemie - Int. Ed.*, **54** (9), 2784–2787.

13. Taglieber, A., Schulz, F., Hollmann, F., Rusek, M., and Reetz, M.T. (2008) Light-Driven Biocatalytic Oxidation and Reduction Reactions : Scope and Limitations. 565–572.

14. Lee, S.H., Choi, D.S., Kuk, S.K., and Park, C.B. (2018) Photobiocatalysis: Activating Redox Enzymes by Direct or Indirect Transfer of Photoinduced Electrons. *Angew. Chemie - Int. Ed.*, **57** (27), 7958–7985.

15. Hollmann, F., Taglieber, A., Schulz, F., and Reetz, M.T. (2007) A light-driven stereoselective biocatalytic oxidation. *Angew. Chemie - Int. Ed.*, **46** (16), 2903–2906.

16. Rauch, M., Schmidt, S., Arends, I.W.C.E., Oppelt, K., Kara, S., and Hollmann, F. (2017) Photobiocatalytic alcohol oxidation using LED light sources. *Green Chem.*, **19** (2), 376–379.

17. Ravelli, D., and Fagnoni, M. (2012) Dyes as Visible Light Photoredox Organocatalysts. *ChemCatChem*, **4** (2), 169–171.

18. Broichhagen, J., and Weck, M. (2010) Strain-Promoted Alkyne Azide Cycloaddition for the Functionalization of Poly(amide)-Based Dendrons and Dendrimers. (24), 3923–3931.

19. Mbua, N.E., Guo, J., Wolfert, M.A., Steet, R., and Boons, G.J. (2011) Strain-Promoted Alkyne-Azide Cycloadditions (SPAAC) Reveal New Features of Glycoconjugate Biosynthesis. *ChemBioChem*, **12** (12), 1912–1921.

20. Boutureira, O., and Bernardes, G.J.L. (2015) Advances in Chemical Protein Modification. *Chem. Rev.*, **115** (5), 2174–2195.

21. Weitzel, K., Chemie, F., Rev, M.S., Introduction, I., and Reference, C. (2011) Bond-Dissociation Energies of Cations — Pushing the. *WHO Libr. Cat. Data*, 221–235.

22. Schoffelen, S., Lambermon, M.H.L., Van Eldijk, M.B., and Van Hest, J.C.M. (2008) Site-specific modification of Candida antarctica lipase B via residue-specific incorporation of a non-canonical amino acid. *Bioconjug. Chem.*, **19** (6), 1127–1131.

23. Gaetke, L.M., and Chow, C.K. (2003) Copper toxicity, oxidative stress, and antioxidant nutrients. *Toxicology*, **189** (1–2), 147–63.

24. Paria, S., and Reiser, O. (2014) Copper in photocatalysis. *ChemCatChem*, **6** (9), 2477–2483.

25. Plass, T., Milles, S., Koehler, C., Szymański, J., Mueller, R., Wießler, M., Schultz, C., and Lemke, E.A. (2012) Amino acids for diels-alder reactions in living cells. *Angew. Chemie - Int. Ed.*, **51** (17), 4166–4170.

26. Zou, H., Li, L., Zhang, T., Shi, M., Zhang, N., Huang, J., and Xian, M. (2018) Biosynthesis and biotechnological application of non-canonical amino acids: Complex and unclear. *Biotechnol. Adv.*, **36** (7), 1917–1927.

27. Link, A.J., Mock, M.L., and Tirrell, D.A. (2003) Non-canonical amino acids in protein engineering. *Curr. Opin. Biotechnol.*, **14** (6), 603–609.

28. Fladischer, P., Weingartner, A., Blamauer, J., Darnhofer, B., Birner-

Gruenberger, R., Kardashliev, T., Ruff, A.J., Schwaneberg, U., and Wiltschi, B. (2018) A Semi-Rationally Engineered Bacterial Pyrrolysyl-tRNA Synthetase Genetically Encodes Phenyl Azide Chemistry. *Biotechnol. J.*, **1800125**, 1800125.

29. Chemla, Y., Ozer, E., Algov, I., and Alfonta, L. (2018) Context effects of genetic code expansion by stop codon suppression. *Curr. Opin. Chem. Biol.*, **46** (Box 1), 146–155.

30. Plass, T., Milles, S., Koehler, C., Szymański, J., Mueller, R., Wießler, M., Schultz, C., and Lemke, E.A. (2012) Amino acids for diels-alder reactions in living cells. *Angew. Chemie - Int. Ed.*, **51** (17), 4166–4170.

31. Holtmann, D., and Hollmann, F. (2016) The Oxygen Dilemma: A Severe Challenge for the Application of Monooxygenases? *ChemBioChem*, 1391–1398.

32. Fitzpatrick, T.B., Amrhein, N., and Macheroux, P. (2003) Characterization of YqjM, an old yellow enzyme homolog from Bacillus subtilis involved in the oxidative stress response. *J. Biol. Chem.*, **278** (22), 19891–19897.

33. Kitzing, K., Fitzpatrick, T.B., Wilken, C., Sawa, J., Bourenkov, G.P., Macheroux, P., and Clausen, T. (2005) The 1.3 Å crystal structure of the flavoprotein YqjM reveals a novel class of old yellow enzymes. *J. Biol. Chem.*, **280** (30), 27904–27913.

34. Okamoto, Y., Köhler, V., Paul, C.E., Hollmann, F., and Ward, T.R. (2016) Efficient in situ regeneration of NADH mimics by an artificial metalloenzyme. *ACS Catal.*, **6** (6), 3553–3557.

35. Fitzpatrick, T.B., Auweter, S., Kitzing, K., Clausen, T., Amrhein, N., and MacHeroux, P. (2004) Structural and functional impairment of an Old Yellow Enzyme homologue upon affinity tag incorporation. *Protein Expr. Purif.*, **36** (2), 280–291.

36. Pesic, M., Fernández-Fueyo, E., and Hollmann, F. (2017) Characterization of the Old Yellow Enzyme Homolog from Bacillus subtilis (YqjM). *ChemistrySelect*, **2** (13), 3866–3871.

37. Bermúdez, E., Ventura, O.N., Eriksson, L.A., and Saenz-Méndez, P. (2014) Improved homology model of cyclohexanone monooxygenase from Acinetobacter calcoaceticus based on multiple templates. *Comput. Biol. Chem.*, **49**, 14–22.

38. Dunn, P.J. (2012) The importance of Green Chemistry in Process Research and Development. *Chem. Soc. Rev.*, **41** (4), 1452–1461.

7 APPENDIX

7.1 LIST OF PRIMERS

name	sequence 5'-3'
1_pSCS-MmOP_T7_CHMO_C-His - primer_CHMO_fwd_58.2	TAATACGACTCACTATAGGGGAATTGTGAGCGGATAACAATTCCCCTCTAGAAATAATTTTGTTTAACTTTAAGAAGGAGATATACCATGTCACAAAAAATGGATTTTGATGCTAT
2_pSCS-MmOP_T7_CHMO_C-His - CHMO_primer_rev_58.2	GATCTATCAACAGGAGTCGAATTAGATCTCAGTGGTGGTGGTGGTG
3_pSCS-MmOP_T7_YqJm_C-His - primer_fastcloning_rev_49.1	CTTTAAGAAGGAGATATACCATGGCCAGAAAATTATTTAC
4_pSCS-MmOP_T7_YqJm_C-His - primer_fastcloning_fwd_49.1	GTAAATAATTTTCTGGCCATGGTATATCTCCTTCTTAAAG
5_pSCS-MmOP_T7_YqJm_C-His - primer_fastcloning_insert_yqjm_rev_	GGTGGTGCTCGAGTGCGGCCGCCCAGCCTCTTTCGTATTG
6_pSCS-MmOP_T7_YqJm_C-His - primer_fastcloning_insert_yqjm_fwd	CAATACGAAAGAGGCTGGGCGGCCGCACTCGAGCACCACC
7_Primer_CHMO_C-His_rv	TCAGTGGTGGTGGTGGTGCTCGAGTGCGGCCGCGGCATTGGCAGGTTGCTTG
8_Primer_CHMO_C-His_fw	ATGTCACAAAAAATGGATTTTGATGC
9_Primer_Gibson_cterm_fw	ATGCCTGCAAGCTGCAGATTAATGGGTCTCTAGAATTTTAATACGACTCACTATAGGGG
10_Primer_Gibson_cterm_rev	GATCTATCAACAGGAGTCGA
11_T7_fwd_primer	TAATACGACTCACTATAGGG
12_pBPA32_sequencing_primer	GAGGTCATTACTGGATCTATCAACAG
13_Hannahs18_CHMOsequencing_Primer	GAAGCGCAAAATTTCATTAAGG
14_TEV_YqjM_fwd	ATGGCCAGAAAATTATTTACAC
15_TEV_YqjM_rev	GAAAACCTGTATTTTCAGGGCGGCCGCCCAGCCTCTTTCGTATTG
16_TEV_fc_YqjM_up_fwd	ATAATTTTGTTTAACTTTAAGAAGGAGATATACCATGGCCAGAAAATTATTTACACC
17_TEV_fc_YqjM_up_rev	GGTGTAAATAATTTTCTGGCCATGGTATATCTCCTTCTTAAAGTTAAACAAAATTAT
18_TEV_fc_YqjM_up_fwd	GCCCTGAAAATACAGGTTTTCGCACTCGAGCACCACC
19_TEV_fc_YqjM_up_rev	GGTGGTGCTCGAGTGCGAAAACCTGTATTTTCAGGGC
20_vector_yqjmtev fwd	GAAAATACAGGTTTTCGCACTCGAGCACCACCAC
21_vector_yqjmtev_rev	GTAAATAATTTTCTGGCCATGGTATATCTCCTTCTTAAAGTTAAACAAAATTATTTC
22_Kan_rev	GGGCTTCCCATACAATCGATAG

23_Nde1_YqjM_qc_fwd	GATATCATATGGCCAGAAAATTATTTAC
24_Nde1_YqjM_qc_rev	CTGGCCATATGATATCTCCTTCTTAAAG
25_Nde1/his_yqjmtev_fwd	GATATCATATGGCCAGAAAATTATTTAC
26_Nde1/his_yqjmtev_rev	GAATTAGATCTCAGTGGTGGTGGTGGTGGTGCT CGAGTGCGAAAACCTGTATTTTCAGG
27_CHMO_R389_fwd	CTATGTGTAGATGGACATTCAAGG
28_CHMO_R389_rev	CATCTACACATAGTTGCCATCGAC
29_CHMO_N156_fwd	GGCATTTAGCAGTTTAAAGGTGAGC
30_CHMO_N156_rev	CTGCTAAATGCCTTTGATGTTTGGC
31_CHMO_E127_fwd	CACCACTTAGTATGGTGATAAGTAC
32_CHMO_E127_rev	CATACTAAGTGGTGACTTCCCAC
33_YqjM_T70_fwd	GAATCTAGGACCAAGACTTAG
34_YqjM_T70_rev	GTCCTAGATTCGTCCTTGAG
35_YqjM_K109_fwd	CGTTAGGCTGAGCTTGAAGG
36_YqjM_K109_rev	CAGCCTAACGTCCGGCATGG
37_YqjM_E335_fwd	GTTCAATACTAGAGAGGCTGG
38_YqjM_E335_rev	CTCTAGTATTGAACAGGGGCC
39_TEV_rev	GAAAACCTGTATTTTCAGGGC
40_pETCHMO_upfwd	GTTTAACTTTAAGAAGGAGATATACCATGTCACAA AAAATGGATTTTGATG
41_pETCHMO_uprev	CATCAAAATCCATTTTTTGTGACATGGTATATCTC CTTCTTAAAGTTAAAC
42_pETCHMO_dwfwd	GCAACCTGCCAATGCCGCGGCCGCACTCG
43_pETCHMO_dwrev	CGAGTGCGGCCGCGGCATTGGCAGGTTGC
44_CHMOsequ_rev	GATATTGGCTTCCATATTG
45_CHMOsequ_fwd	CTTTGGCCTGAATGAAAG
46_YqjMsequ_rev	CTGCTCCTTCATCCATTTTG
47_YqjMsequ_fwd	CAGAAAAAGTAAAAGAAAC
48_P5CHMO_upfwd	GAGGAGAAATTAACTATGTCACAAAAAATGGATT TTG

49_P5CHMO_uprev	CAAAATCCATTTTTTGTGACATAGTTAATTTCTCC TC
50_P5CHMO_dwrev	GTCGAATTAGATCTTCAGTGGTGGTGGTG
51_P5CHMO_dwfwd	CACCACCACCACTGAAGATCTAATTCGAC
52_Pm_242_fw	AAATATGTGCAAGGCCCTGATG
53_Pm_242_rv	CACATATTTTTTCTTGATTTCTAGCG
54_Pm_16xx_fw	CCGCACTCGAGCACCACCACCACCACCACT
55_Pm_16xx_rv	GTGGTGCTCGAGTGCGGCCGCGGCATTGGC

7.2 PLASMIDS

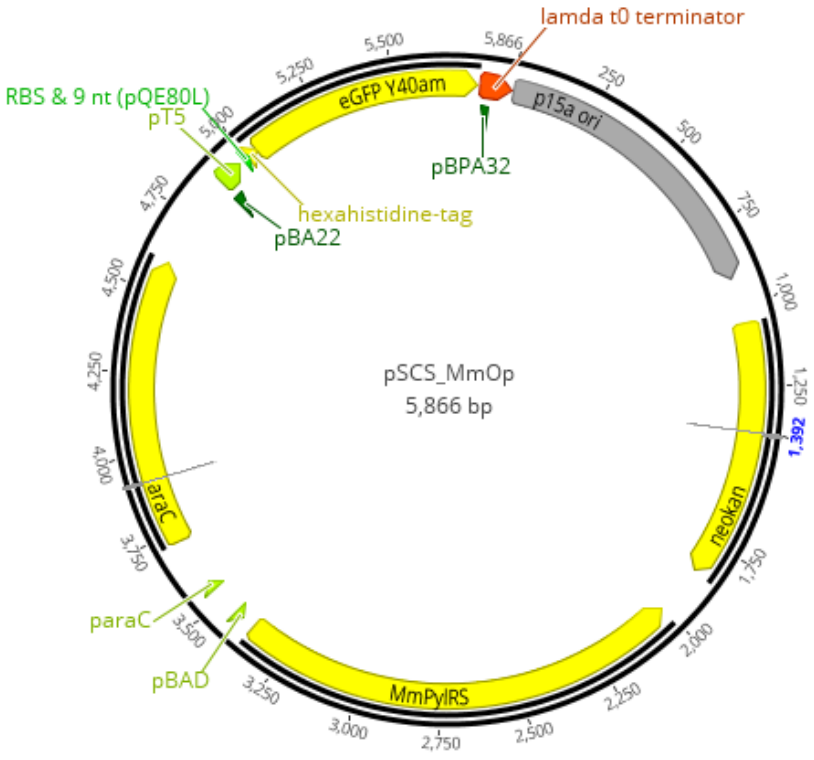

Figure 27: Vector map of pSCS_MmOp generated using geneious.

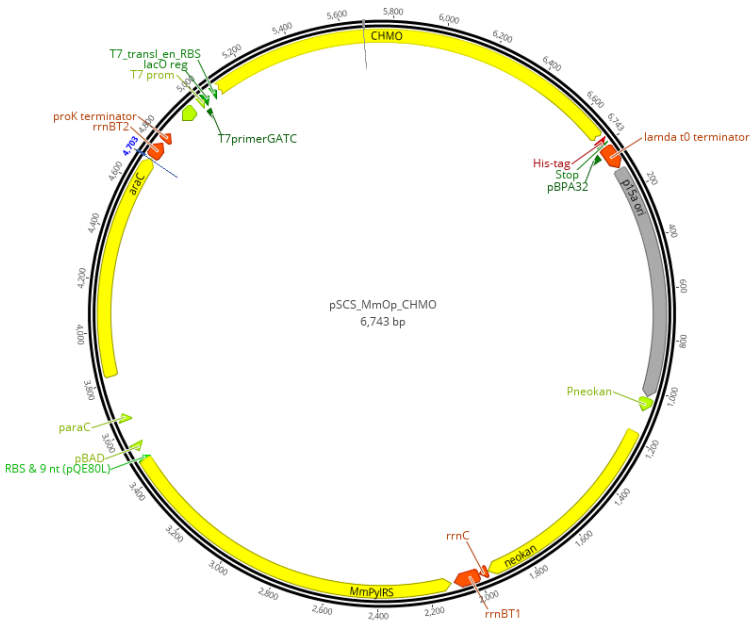

Figure 28: Vector map of pSCS_MmOp_CHMO_T7 generated using geneious.

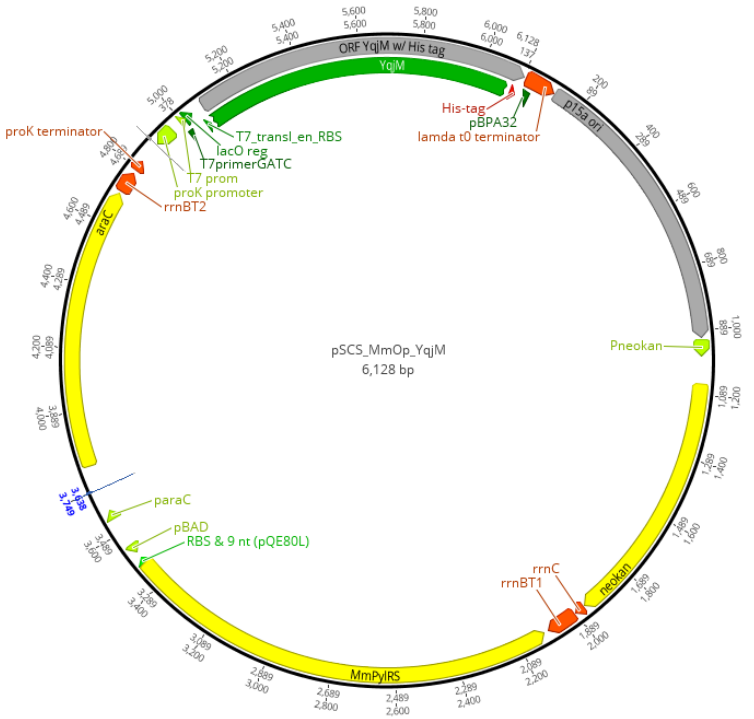

Figure 29: Vector map of pSCS_MmOp_YqjM_T7 generated using geneious.

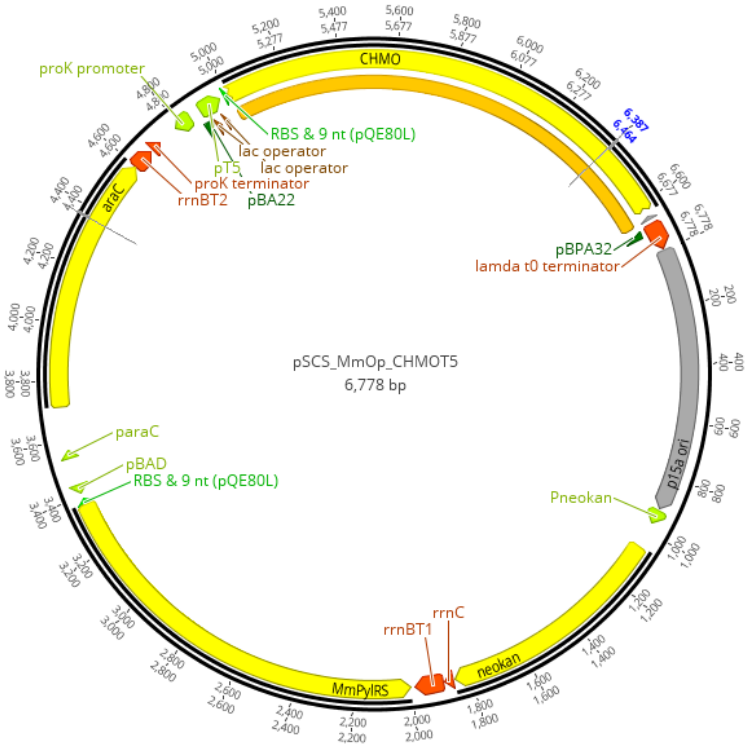

Figure 30: Vector map of pSCS_MmOp_CHMO_T5 generated using geneious.

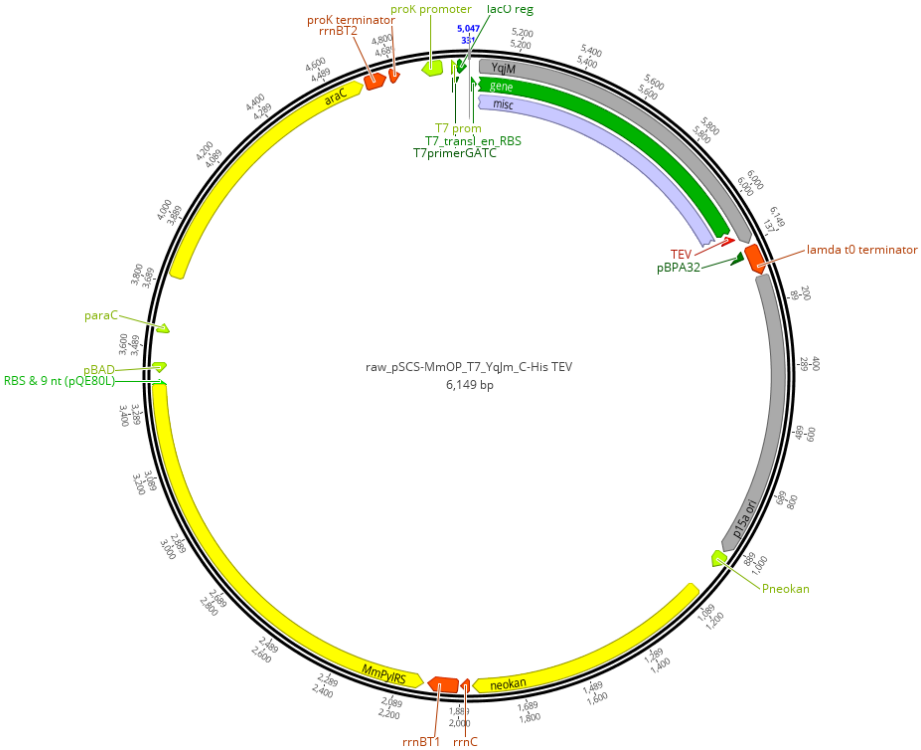

Figure 31: Vector map of pSCS_MmOp_YqjMTEV_T7 generated using geneious.

7.3 PROTEIN SEQUENCES

Below the sequences for CHMO and YqjM are shown. The red marked amino acids cannot be used, the yellow marked are possible loci for a replacement with azidolysine. The chosen positions for the further experiment are the amino acids in yellow marked with boxes.

CHMO:

MSQKMDFDAIVIGGGFGGLYAVKKBsmGILRDELELKVQAFDKATDVAGTWYWNRYPGALTDTETHL
YCYSWDKELLQSLEIKKKYVQGPDVRKYLQQVAEKHDLKKSYQFNTAVQSAHYNEADALWEVTTEY
GDKYTARFLITALGLLSAPNLPNIKGINQFKGELHHTSRWPDDVSFEGKRVGVIGTGSTGVQVITAVAP
LAKHLTVFQRSAQYSVPIGNDPLSEEDVKKIKDNYDKSLGWCMNSALAFALNESTVPAMSVSAEERK
AVFEKAWQTGGGFRFMFETFGDIATNBstXIMEANIEAQNFIKGKIAEIVKDPAIAQKLMPQDLYAKRPL
CDSGYYNTFNRDNVRLEDVKANPIVEITENGVKLENGDFVELDMLICATGFDAVDGNYVRMDIQGKN
GLAMKDYWKEGPSSYMGVTVNNYPNMFMVLGPNGPFTNLPPSIESQVEWISDTIQYTVENNVESIEA
TKEAEEQWTQTCANIAEMTLFPKAQSWIFGANIPGKKNTVYFYLGGLKEYRTCASNCKNHAYEGFDIQ
LQRSDIKQPANA*

YqjM:

MARKLFTPITIKDMTLKNRIVMSPMCMYSSHEKDGKLTPFHMAHYISRAIGQVGLIIVEASAVHpaI/
KspANPQGRITDQDLGIWSDEHIEGFAKLTEQVKEQGSKIGIQLAHAGRKAELEGDIFAPSAIAFD
EQSATPVEMSAEKVKETVQEFKQAAARAKEAGFDVIEIHAAHGYLIHEFLSPLSNHRTDEYGGSP
ENRYRFLREIIDEVKQVWDGPLFVRVSASDYTDKGLDIADHIGFAKWMKEQGVDLIDCSSGALVH
ADINVFPGYQVSFAEKIREQADMATGAVGMITDGSMAEEILQNGBtrI/AjiI/BmgBIRADLIFIGRELL
RDPFFARTAAKQLNTEIPAPVQYERGW

7.4 SEQUENCING OF AMBER STOP CODON VARIANTS

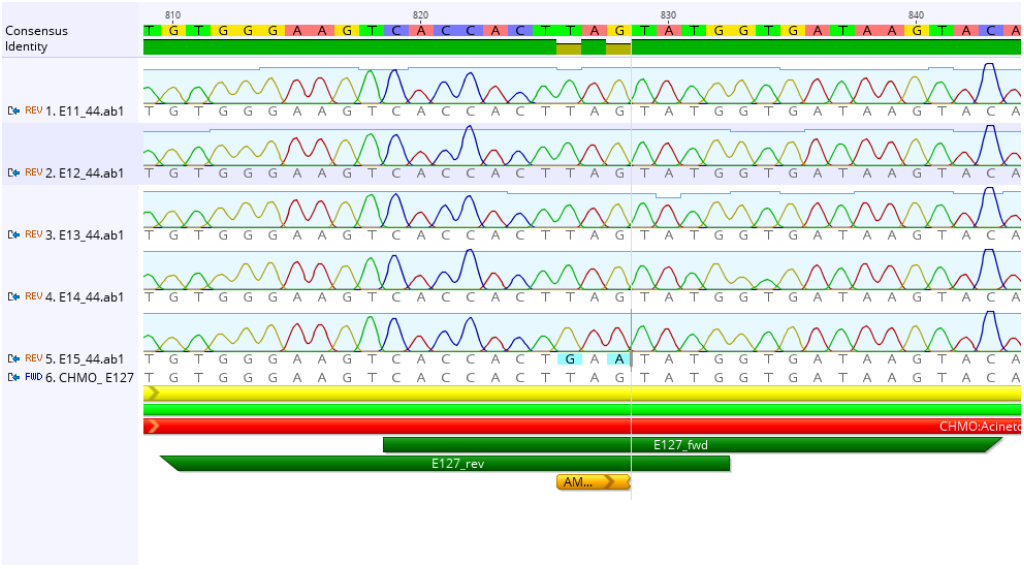

Figure 32: Confirmation of successful generation of the AMBER stop codon in *chmo* at position E127. The sequenced construct of Position 4 (4. E14) was used in further experiments. Figure created with geneious.

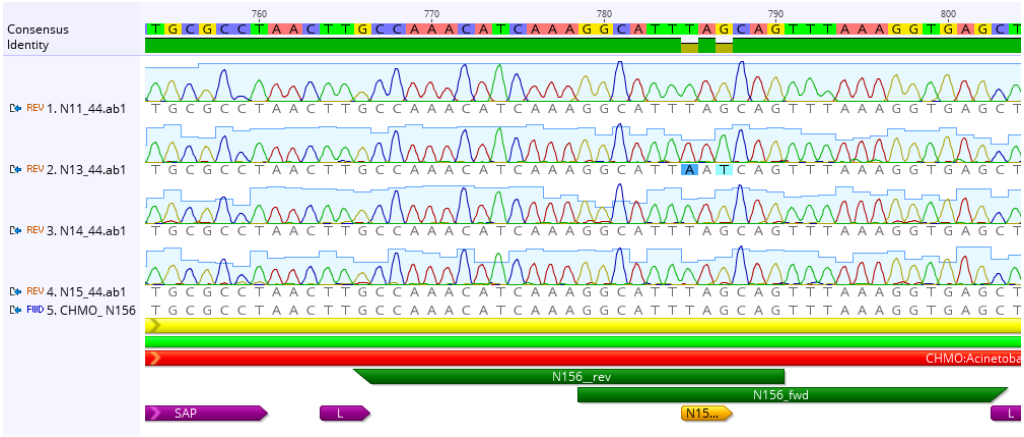

Figure 33: Confirmation of successful generation of the AMBER stop codon in *chmo* at position N156. The sequenced construct of Position 4 (4. N14) used in further experiments. Figure created with geneious.

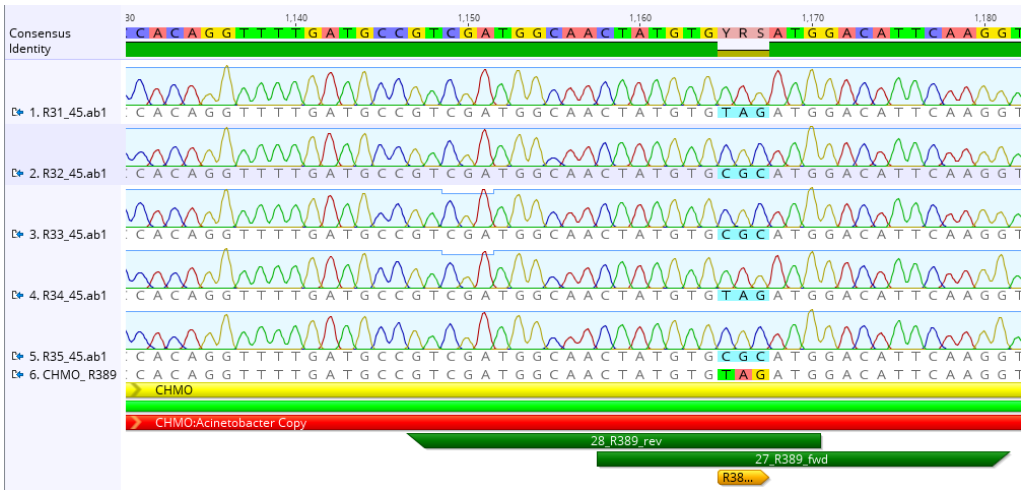

Figure 34: Confirmation of successful generation of the AMBER stop codon in *chmo* at position R389. The sequenced construct of Position 4 (4. R14) was used in further experiments. Figure created with geneious.

Figure 35: Confirmation of successful generation of the AMBER stop codon in *yqjm* at position T70. Figure created with geneious.

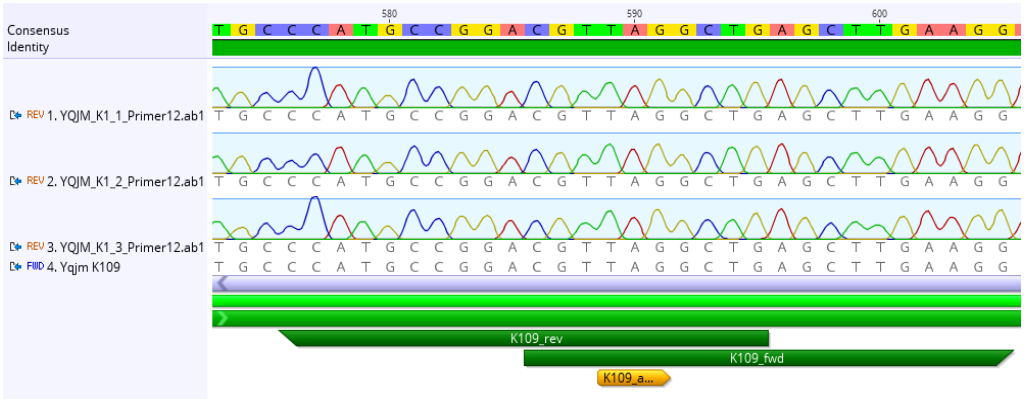

Figure 36: Confirmation of successful generation of the AMBER stop codon in *yqjm* at position K109. Figure created with geneious.

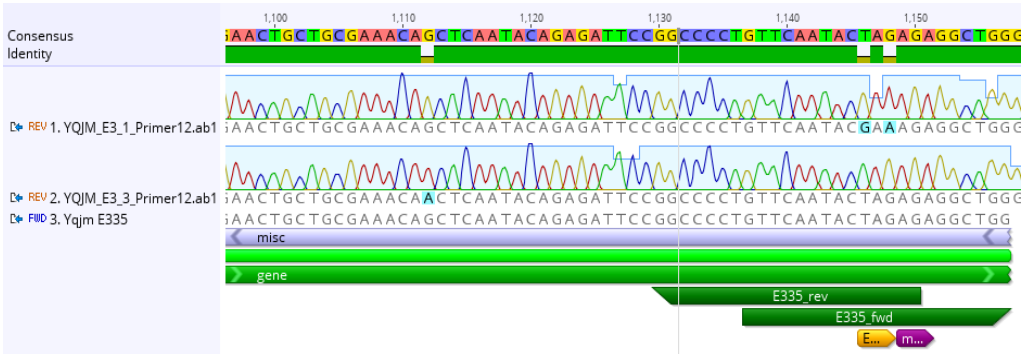

Figure 37: Confirmation of successful generation of the AMBER stop codon in *yqjm* at position E335. Figure created with geneious.

7.5 AGAROSE GEL ELECTROPHORESIS

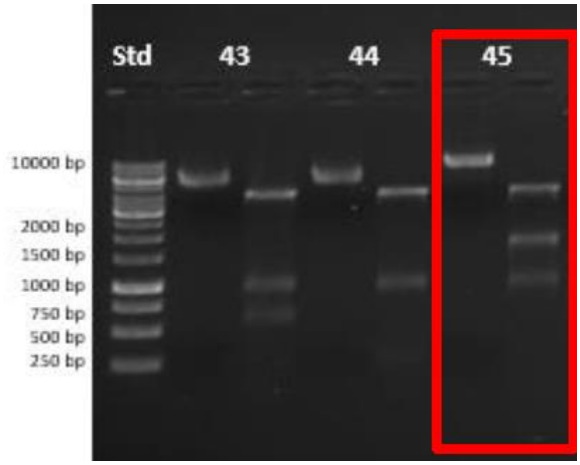

Figure 38: Confirmation of pSCS_MmOp_CHMO_T7 by restriction analysis using the restriction enzymes *Xba*I and *Bgl*II.

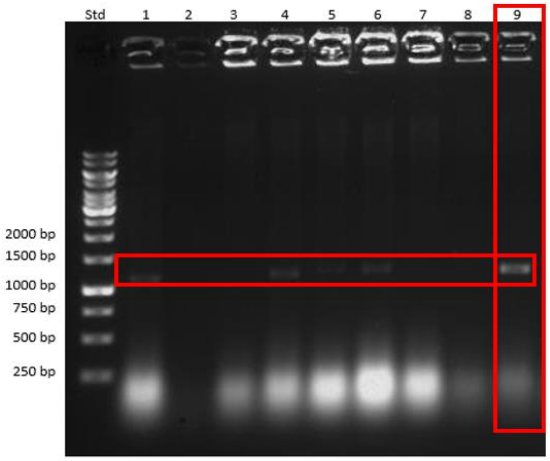

Figure 39: Shown is the result of the colony PCR of *E. coli* TOP10 carrying pSCS_MmOp_YqjMTEV_T7 construct.

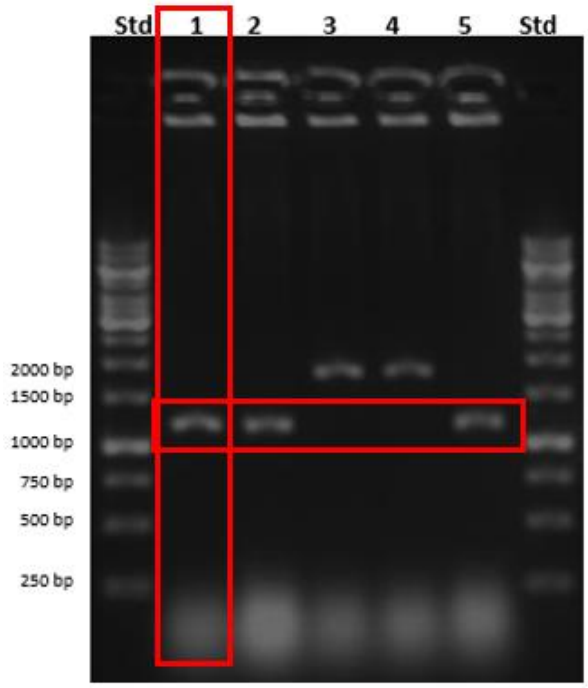

Figure 40: Shown is the result of the colony PCR of *E. coli* TOP10 carrying pSCS_MmOp_YqjM_T7 construct.

7.6 GC-FID ANALYSIS

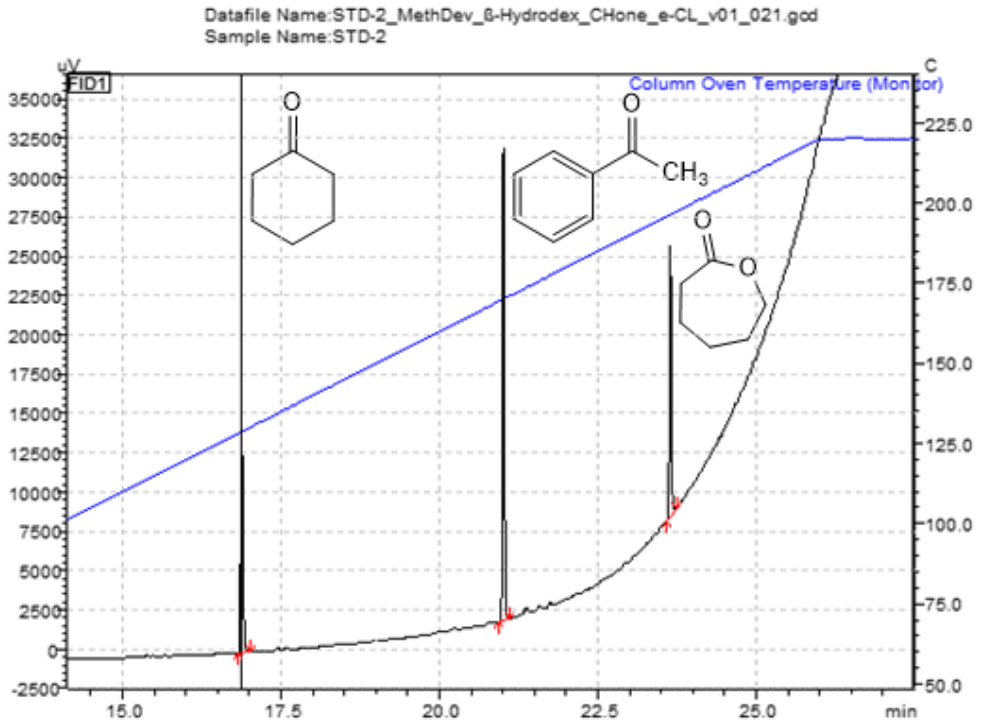

Figure 41: Standard measurements for GC-FID analysis determination 2 mM of cyclohexanone and ε-caprolactone. Acetophenone was used as internal standard.

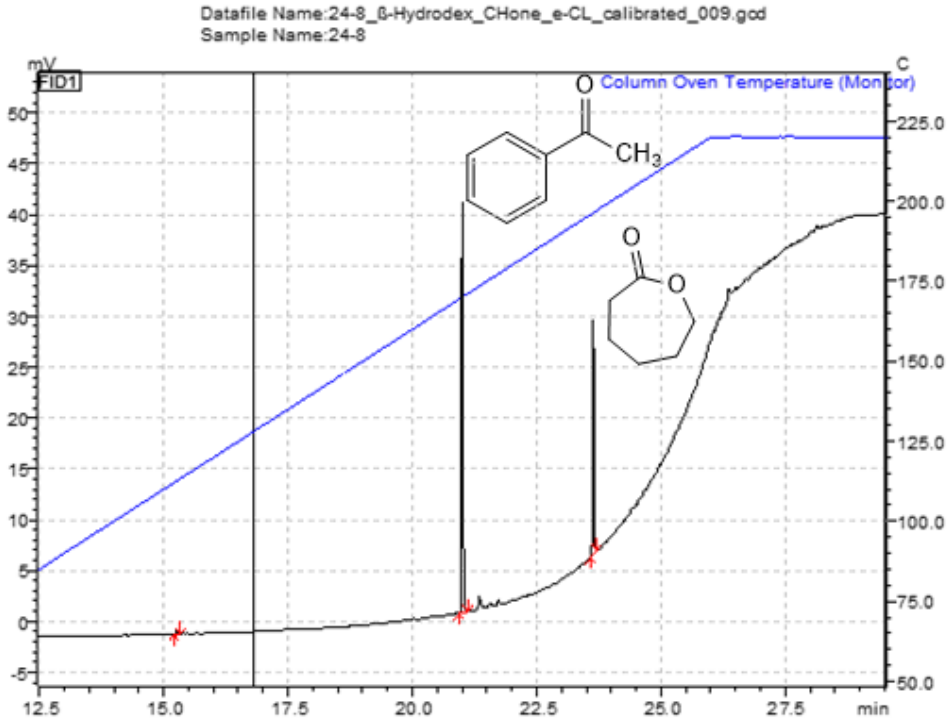

Figure 42: Chromatogram of GC-FID analysis of sample taken from conversion of cyclohexanone to ε-caprolactone catalyzed by CHMO, using NADPH as cofactor. Acetophenone was used as internal standard and no cyclohexanone was determined after 24 hours.

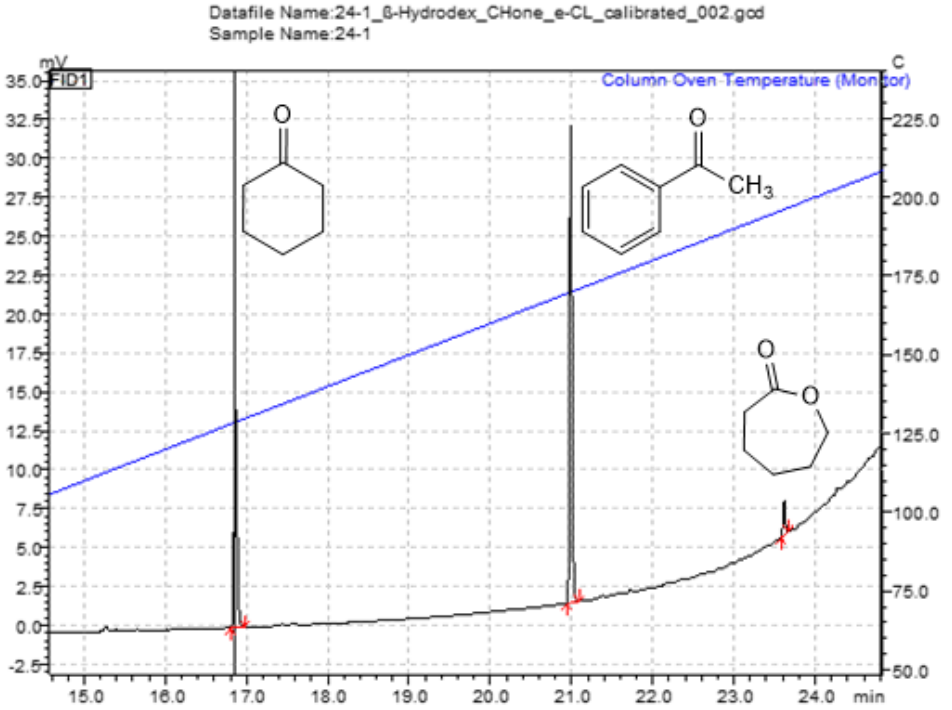

Figure 43: Chromatogram of GC-FID analysis of sample taken from conversion of cyclohexanone to ε-caprolactone catalyzed by CHMO, using blue light for light-driven photobiocatalysis. Acetophenone was used as internal standard.